Neuroscience

POMC neurons control fertility through differential signaling of MC4R in Kisspeptin neurons

Reviewed Preprint
v1 • September 11, 2024
Not revised

Rajae Talbi, Todd L Stincic, Kaitlin Ferrari, Choi Ji Hae, Karol Walec, Elizabeth Medve, Achi Gerutshang, Silvia León, Elizabeth A McCarthy, Oline K Rønnekleiv, Martin J Kelly, Víctor M Navarro

Harvard Medical School, Boston, MA, USA • Division of Endocrinology, Diabetes and Hypertension, Department of Medicine, Brigham and Women's Hospital, Boston, MA, USA • Division of Neuroscience, Oregon National Primate Research Center, Beaverton, OR, USA • Department of Chemical Physiology and Biochemistry, Oregon Health & Science University, Portland, OR, USA • Harvard Program in Neuroscience, Boston, MA, USA

Abstract

Inactivating mutations in the melanocortin 4 receptor (*MC4R*) gene cause monogenic obesity. Interestingly, female patients also display various degrees of reproductive disorders, in line with the subfertile phenotype of MC4RKO female mice. However, the cellular mechanisms by which MC4R regulates reproduction are unknown. Kiss1 neurons directly stimulate gonadotropin-releasing hormone (GnRH) release through two distinct populations; the $Kiss1^{ARH}$ neurons, controlling GnRH pulses, and the sexually dimorphic $Kiss1^{AVPV/PeN}$ neurons controlling the preovulatory LH surge. Here, we show that *Mc4r* expressed in Kiss1 neurons is required for fertility in females. *In vivo*, deletion of *Mc4r* from Kiss1 neurons in female mice replicates the reproductive impairments of MC4RKO mice without inducing obesity. Conversely, reinsertion of *Mc4r* in Kiss1 neurons of MC4R null mice restores estrous cyclicity and LH pulsatility without reducing their obese phenotype. *In vitro*, we dissect the specific action of MC4R on $Kiss1^{ARH}$ vs $Kiss1^{AVPV/PeN}$ neurons and show that MC4R activation excites $Kiss1^{ARH}$ neurons through direct synaptic actions. In contrast, $Kiss1^{AVPV/PeN}$ neurons are normally inhibited by MC4R activation except under elevated estradiol levels, thus facilitating the activation of $Kiss1^{AVPV/PeN}$ neurons to induce the LH surge driving ovulation in females. Our findings demonstrate that $POMC^{ARH}$ neurons acting through MC4R, directly regulate reproductive function in females by stimulating the "pulse generator" activity of $Kiss1^{ARH}$ neurons and restricting the activation of $Kiss1^{AVPV/PeN}$ neurons to the time of the estradiol-dependent LH surge, and thus unveil a novel pathway of the metabolic regulation of fertility by the melanocortin system.

eLife assessment

The study presents **compelling** evidence that the melanocortin system originating in the arcuate nucleus of the hypothalamus plays a crucial role in puberty onset, representing a significant advance in our understanding of reproductive biology. The work, which represents a **fundamental** advance, employs innovative approaches and benefits from the combined expertise of two respected laboratories, enhancing the robustness of the findings. Given the potential impact on human health and the strength of the evidence presented, this work will likely influence the field substantially and may inform future clinical applications.

https://doi.org/10.7554/eLife.100722.1.sa4

Introduction

Obesity rates have skyrocketed in Western societies in the last decades, resulting in an alarming rise in comorbidities that place a significant burden on healthcare systems. The increase in obesity correlates with a decrease in fertility rates, leading to conception challenges that are experienced by approximately 15% of couples in the United States currently [1].

The melanocortin 4 receptor (MC4R) binds α-melanocyte stimulating hormone (αMSH), an agonist product of the pro-opiomelanocortin (*Pomc*) gene, and the inverse agonist of the agouti-related peptide (AgRP) to regulate food intake and energy expenditure [2,3]. While the role of MC4R on food intake is largely mediated by neurons located in the paraventricular nucleus of the hypothalamus (PVN) [4], its expression in the brain is widespread [5] with the specific function of the different MC4R-expressing neurons in areas beyond the PVN remaining to be fully explored. Inactivating mutations in *MC4R* are a leading cause of monogenic obesity in humans and mice [6]. Scant evidence in humans shows an association between *MC4R* mutations and higher incidence of hypogonadotropic hypogonadism (HH) [7], alterations in the timing of puberty onset [8], and polycystic ovary syndrome (PCOS) [9]; however, conflicting reports exist [6]. Therefore, the role of MC4R signaling in reproductive function in humans remains controversial despite the clear association found in mice. Supporting this role of MC4R, *Mc4r* null mice display an array of reproductive abnormalities that largely affects females, characterized by irregular estrous cycles, disrupted luteinizing hormone (LH) secretion, reduced corpora lutea and reduced fertility [10–12]. Further evidence from mice demonstrates that MC4R agonists robustly increase LH release in a kisspeptin-dependent manner [13].

Kisspeptin is the most potent gonadotropin releasing hormone (GnRH) secretagogue known to date and it is mainly produced in two distinct neuronal populations. Kiss1 neurons of the arcuate nucleus of the hypothalamus ($Kiss1^{ARH}$), present in both sexes, control the pulsatile (tonic) release of GnRH, and sex steroids attenuate their release of kisspeptin. Kiss1 neurons of the anteroventral periventricular continuum area ($Kiss1^{AVPV/PeN}$), are predominantly present in females, and are responsible for generating the preovulatory GnRH/LH surge essential for ovulation [14]. Despite these critical roles of both populations of Kiss1 neurons for reproduction, the underlying mechanisms that determine how each Kiss1 population responds differently to sex steroids to regulate the GnRH tonic vs surge release remains unresolved.

In rodents, compelling evidence indicates a close interaction between Kiss1 neurons and the melanocortin system: 1) fibers from POMC neurons in the arcuate nucleus ($POMC^{ARH}$) project to and juxtapose $Kiss1^{ARH}$ neurons [13]; 2) the melanocortin signaling through MC4R contributes to

the permissive role of leptin on puberty onset [13,15,16]; and 3) MC4R expression on both Kiss1^{ARH} [17–19] and Kiss1$^{AVPV/PeN}$ [17,20]. Altogether, this evidence suggests a clear role for MC4R in Kiss1 neurons, in the control of reproductive maturation and fertility.

In this study, we investigated the contribution of MC4R signaling versus obesity *per se* in the etiology of the reproductive impairments observed in *Mc4r* null mice, which could explain similar impairments observed in humans. Using genetic mouse models with specific deletion or reinsertion of *Mc4r* in Kiss1 neurons, we show that MC4R action in Kiss1 neurons is necessary for normal reproductive function in female mice. Whole cell voltage clamp recordings evidenced an excitatory action of MC4R on Kiss1^{ARH} neurons and an estradiol-dependent inhibitory action on Kiss1$^{AVPV/PeN}$ neurons, with important implications for the timing of the preovulatory LH surge.

Results

Mc4r within Kiss1 neurons determines the timing of puberty onset in females

The expression of *Mc4r* within Kiss1^{ARH} and Kiss1$^{AVPV/PeN}$ neurons has already been described elsewhere [17–20], suggesting a role for MC4R in the regulation of fertility. To further investigate the specific role of MC4R in Kiss1 neurons, we generated a Kiss1-specific MC4R knockout mouse model (Kiss1-MC4RKO). The specific deletion of *Mc4r* from Kiss1 neurons, as well as the absence of global recombination, were confirmed through RNAscope. While Kiss1 neurons of Kiss1-MC4RKO mice lack *Mc4r* transcript compared to their control littermates (**Figure S*1A***), *Mc4r* was detectable in the PVN of all mice, which is a major site of *Mc4r* expression in the brain in the regulation of metabolism, therefore supporting the specific deletion of *Mc4r* only within Kiss1 neurons (**Figure S*1B***).

Puberty onset was assessed daily from weaning age through the monitoring of vaginal opening (VO) and first estrus (FE). Kiss1-MC4RKO females showed a significant advancement in the age of VO (P=0.0150, Kiss1-MC4RKO: 24.67± 0.3978 vs controls: 26.32±0.5301) and FE (P=0.0341, Kiss1-MC4RKO: 32.63±1.489 vs controls: 37.84±1.903) compared to their littermate controls (**Figure 1A, B**). Body weight of Kiss1-MC4RKO females at the age of puberty onset was similar between groups (P=0.2596, Kiss1-MC4RKO: 12.41±0.3041 vs controls: 12.89±0.2631) (**Figure 1*C***). These data suggest that melanocortin signaling on Kiss1 neurons participates in the timing of puberty onset in females. Since the role of the melanocortin system on puberty onset is largely unexplored, we evaluated the expression profile of the main components of this system in the hypothalami of WT female mice at postnatal days (PND) 10, 15, 22 and 30. Interestingly, expressions of *Agrp*, *Mc3r* and *Mc4r* were significantly lower at the time of puberty onset (PND30) compared to earlier developmental ages (**Figure 1*D***). This suggests that a decrease in the hypothalamic melanocortin tone drives puberty onset, in line with the advancement in the age of VO and FE observed in Kiss1-MC4RKO female mice (**Figure 1*A, B***).

MC4R in Kiss1 neurons is required for female reproduction

Because Kiss1-MC4RKO females showed altered puberty onset, we further investigated their reproductive phenotype. Interestingly, Kiss1-MC4RKO female mice displayed normal BW throughout the time of the study (up to PND150) (**Figure 2*A***); however, they presented with irregular estrous cycles with predominantly more time spent in diestrus (P=0.0001) and less time spent in estrus (P<0.0001) than their control littermates (**Figure 2*B, C***). The assessment of the pulsatile release of LH every 10 min over 180 min revealed no change in the total number of pulses between groups but a significant increase in basal LH release (P=0.0368) in Kiss1-MC4RKO female mice (0.426±0.036) compared to controls (0.339±0.026) (**Figure 2*D-H***). The analysis of the

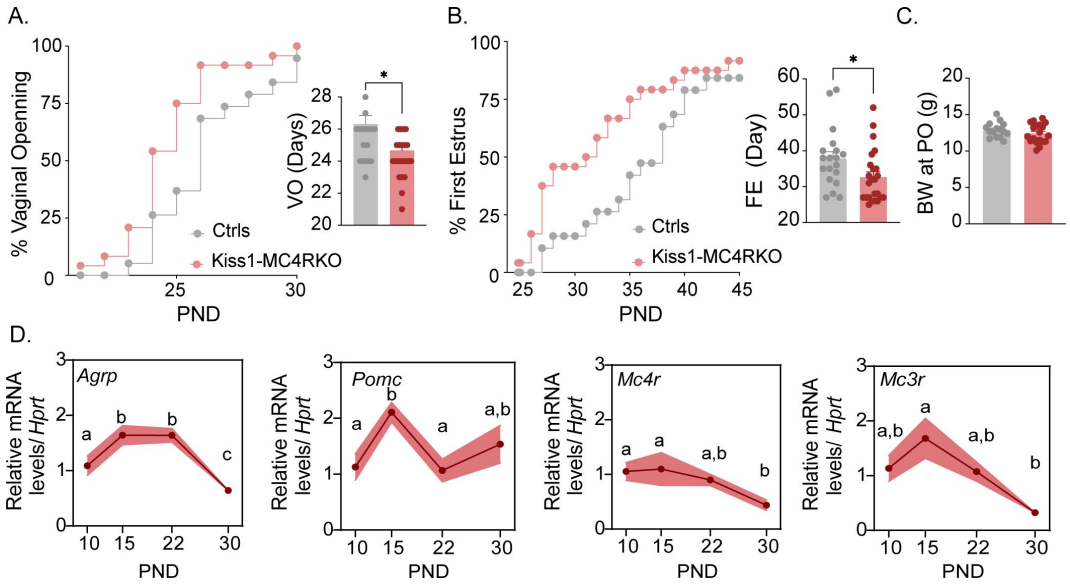

Figure 1.

***Mc4r* expressed in Kiss1 neurons determines the timing of puberty onset.**

Kiss1-MC4RKO females display advanced puberty onset, assessed by daily monitoring of vaginal opening **(A)** and first estrus **(B)**, as documented by cumulative percent and mean age of animals at vaginal opening **(A)** and first estrus **(B)** in Kiss1-MC4RKO females (n=24) compared to WT littermates (n=19). *p<0.05 by Student's t-test. Data presented as the mean± SEM. **(C)** Female Kiss1-MC4RKO (n=19) have normal body weight at the time of puberty onset compared to their WT littermates (n=15). **(D)** Ontogeny expression of melanocortin genes (*Agrp*, *Pomc*, *Mc4r and Mc3r*) in the ARH of WT female mice at different postnatal pre-pubertal and pubertal ages: P10, P15, P22 and P30, normalized to the housekeeping gene *Hprt*. (*n values*: females at P10 (n=6), P15 (n=6), P22 (n=6), and P30 (n=5)). Groups with different letters are significantly different (p<0.05), as determined by one-way ANOVA followed by the Student-Newman-Keuls test. Data presented as the mean± SEM.

gene expression of the "KNDy" systems in the ARH, which control the GnRH pulse generator [14], revealed normal expression levels of *Kiss1*, *Tac2* and *Tacr3*, but significantly lower expression of *Pdyn* (P=0.0067, Kiss1-MC4RKO: 0.781±0.0384 vs controls: 1.000±0.0190) (**Figure 2*I-L***). The conserved expression of *Kiss1*, *Tac2* and *Tacr3* correlates with the preserved LH pulse frequency and amplitude in Kiss1-MC4RKO mice, while the lower inhibitory tone of dynorphin (**Figure 2*I***) correlates with the higher basal LH levels (**Figure 2*E***). To assess the contribution of MC4R signaling in Kiss1 neurons to the induction of ovulation through the preovulatory LH surge, Kiss1-MC4RKO females and control littermates were submitted to an LH surge induction protocol that showed the LH surge was significantly blunted in the Kiss1-MC4RKO females (P=0.0091), while the protocol clearly evoked the expected afternoon rise of LH in control mice (**Figure 2*M***). In line with these findings, the ovaries of Kiss1-MC4RKO females displayed fewer corpora lutea, markers of recent ovulation (P=0.0054, Kiss1-MC4RKO: 0.800±0.374 vs controls: 2.80±0.374), in addition to increased cystic follicles (P=0.0337, Kiss1-MC4RKO: 1.60±0.400 vs controls: 0.400±0.244) (**Figure 2*N-P***), which correlate with decreased fertility as observed by the extended time to deliver pups (*i.e.* longer time to get pregnant) (P=0.0030, Kiss1-MC4RKO: 30.30±4.600 vs controls: 20.88±0.2266), and fewer pups per litter (P=0.0095, Kiss1-MC4RKO: 6.667±0.5528 vs controls: 8.444±0.242) (**Figure 2*S, T***).

The increase in serum LH levels and decreased ovulation observed in the Kiss1-MC4RKO females is reminiscent of polycystic ovary syndrome (PCOS) mouse models [21,22]. Thus, we investigated whether Kiss1-MC4RKO females display a PCOS-like phenotype. We analyzed circulating levels of testosterone (T) and anti-müllerian hormone (AMH), which are frequently elevated in PCOS models [23]. The Kiss1-MC4RKO females expressed normal T and AMH levels compared to control mice in diestrus (**Figure 2*Q, R***). Thus, we can exclude a PCOS-like reproductive phenotype mediated by the lack of melanocortin signaling on Kiss1 neurons.

Re-insertion of MC4R in Kiss1 neurons of MC4RKO mice improves reproductive function

Kiss1-MC4RKO females displayed reproductive abnormalities resembling those described in MC4RKO females [10–12]. Thus, we hypothesized that the reproductive defects described for the MC4RKO mice would be, at least in part, due to the absence of MC4R signaling in Kiss1 neurons. To further investigate this hypothesis, we generated mice that do not express *Mc4r* anywhere (MC4R-LoxTB, *i.e.* MC4RKO) or that express *Mc4r* only in Kiss1 neurons (*Kiss1-cre:MC4R-loxTB*). The specific re-insertion of *Mc4r* within Kiss1 neurons in the *Kiss1-cre:MC4R-loxTB* mice was confirmed through RNAscope (**Figure S2*A*).** *Mc4r* expression was not detected in the PVN of these mice (**Figure S2*B***), and it was only detected in Kiss1 neurons in the *Kiss1-cre:MC4R-loxTB* mice. Puberty onset was assessed daily from weaning age through the monitoring of vaginal opening (VO) and first estrus (FE). MC4R-LoxTB and *Kiss1-cre:MC4R-loxTB* female mice displayed normal timing of puberty onset compared to their control littermates, as assessed by VO (P=0.104, MC4R-LoxTB: 30.86±1.908 vs *Kiss1-cre:MC4R-loxTB: 30.09*±1.004 vs controls: 27.57±0.8168), and FE (P=0.8472, MC4R-LoxTB: 35.14±2.463 vs *Kiss1-cre:MC4R-loxTB: 34.55*±1.648 vs controls: 35.80±0.8406) (**Figure 3*A***), despite displaying significantly higher body weight at the time of puberty onset (P=0.0001, MC4R-LoxTB: 15.49±0.5078 vs *Kiss1-cre:MC4R-loxTB:* 15.54±0.40 vs Controls: 13.29±0.30) (**Figure 3*B***). As expected, MC4R-LoxTB females (MC4RKO) displayed increased body weight (**Figure 3C**) and an array of reproductive impairments that included: irregular estrous cycles with significantly more days in diestrus (P=0.0016) and fewer days in estrus (P=0.0317) compared to controls (**Figure 3*D, E***), significantly higher serum LH levels characterized by higher basal (P=0.0882, MC4R-LoxTB: 0.48±0.02 vs Controls: 0.37±0.06) and amplitude levels per LH pulse (P=0.0102, MC4R-LoxTB: 0.73±0.009 vs Controls: 0.58±0.07) (**Figure 3*F-J***), and fewer corporal lutea (P=0.0366, MC4R-LoxTB: 0.80±0.80 vs Controls: 4.20±1.15) (**Figure 3*K, L***), recapitulating the same reproductive phenotype observed in Kiss1-MC4RKO mice despite the differences in BW. Re-introduction of MC4R into Kiss1 neurons in *Kiss1-cre:MC4R-loxTB* mice completely recovered estrous cyclicity, which was similar to controls (diestrus: P=0.1932,

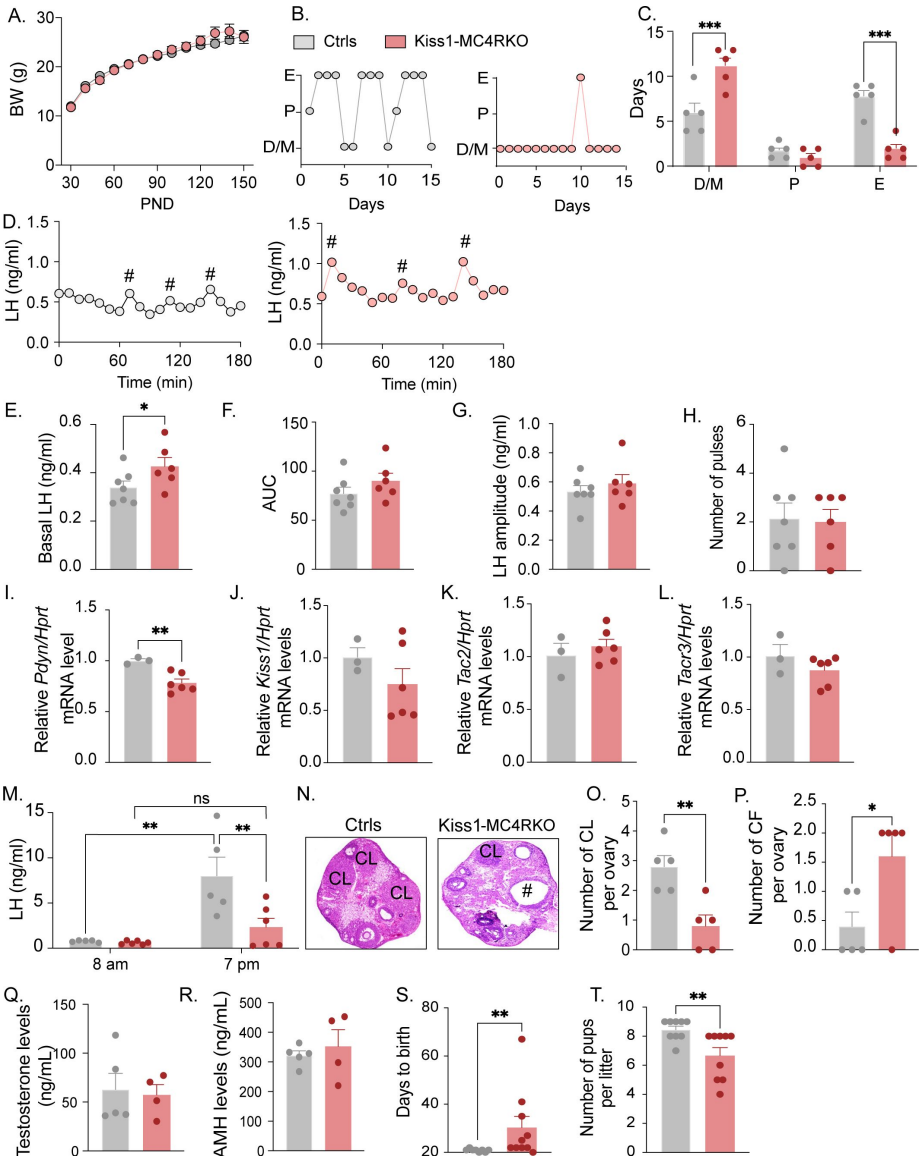

Figure 2.

Deletion of MC4R from Kiss1 neurons impairs fertility in Kiss1-MC4RKO females.

(A) Female Kiss1-MC4RKO (n=19) have normal body weight from weaning and until post-natal day (PND) 150 compared to their WT littermates (n=15). **(B)** Representative examples of estrous cycles in Kiss1-MC4RKO and control females (n=5/group) assessed by daily vaginal cytology for 15 days. **(C)** Kiss1-MC4RKO females displayed irregular estrous cycles with a longer time in diestrus and a shorter time in estrus compared to control females. *** P < 0.001 Two-way ANOVA. **(D)** Pattern of LH pulsatility was analyzed in gonad intact Kiss1-MC4RKO (n=6) and control (n=7) females. # Represents LH pulses. **(E)** Basal LH, **(F)** LH total secretory mass assessed by area under the curve (AUC), **(G)** LH pulse amplitude and **(H)** Total number of pulses /180 min were analyzed. *p<0.05 by Student's t-test. The expression of the KNDy genes *Pdyn* **(I)**, *Kiss1* **(J)**, *Tac2* **(K)** and *Tacr3* **(L)**, was assessed in the ARH of adult Kiss1-MC4RKO (n=6) and control (n=3) females. **p<0.01 by Student's t-test. Data presented as the mean± SEM. **(M)** Kiss1-MC4RKO (n=6) and control (n=5) females were subjected to an LH surge induction protocol. LH samples were collected in the morning (AM [8 a.m.]) and evening (PM [7 p.m.]) after lights off. **P < 0.01, Two-way ANOVA followed by Bonferroni *post hoc* test. **(N)** Ovarian histology shows a decrease in the number of corpora lutea (CL, **O**) and increase in the number of cystic follicles (CF, **P**) of Kiss1-MC4RKO compared to controls(n=5/group). # represents cystic follicles. Serum levels of Testosterone **(Q)** and AMH **(R)** in adult gonad intact Kiss1-MC4RKO and control females (n=5/group). Student t test for unpaired samples. Data presented as the mean± SEM. Kiss1-MC4RKO females display impaired fertility characterized by increased time to deliver pups **(S)** and decreased number of pups per litter **(T)**, (n=9/group). *p<0.05 by Student's t-test. Data presented as the mean± SEM.

proestrus: P=0.8262, estrus: P=0.0547, compared to controls) (**Figure 3*D, E***) despite *Kiss1-cre:MC4R-loxTB* mice showing the same degree of obesity as MC4R-LoxTB mice (**Figure 3*C***), indicating that obesity *per se* was not mediating the irregular estrous cycles in MC4RKO mice. As indicated above, MC4R-LoxTB mice display higher overall circulating LH levels, and this feature was also recovered by the re-insertion of MC4R in Kiss1 neurons of *Kiss1-cre:MC4R-loxTB* mice (basal LH: 0.32±0.044, LH amplitude: 0.48±0.04, LH pulses/180min: 2.75±0.67 and AUC: 70.62±7.156 compared to controls: 80.36±9.058 compared to controls) (**Figure 3*G-J***), further confirming that the melanocortin action on Kiss1 neurons is required for the normal control of gonadotropin release. Despite these significant improvements in reproductive function, *Kiss1-cre:MC4R-loxTB* mice presented fewer corpora lutea than controls (0.80±0.80), similar to MC4R-LoxTB mice, suggesting that an ovulatory impairment still persists (**Fig. 3*K, L***). While tonic LH release and estrous cyclicity are predominantly controlled by Kiss1^{ARH} neurons, ovulation is mediated by the induction of the preovulatory LH surge by Kiss1$^{AVPV/PeN}$ neurons. It is possible that the metabolic signals derived from their obese phenotype, and/or the absence of the direct action of MC4R in GnRH neurons [15,24] prevents the complete recovery of ovulation in *Kiss1-cre:MC4R-loxTB* mice. Both genetic models displayed significantly lower T (MC4R-LoxTB: 28.50±6.20 vs *Kiss1-cre:MC4R-loxTB:* 31.22±3.90 vs Controls: 62.84±16.53) and AMH (MC4R-LoxTB: 150.6±22.00 vs *Kiss1-cre:MC4R-loxTB:* 146.9±10.83 vs Controls: 321.8±15.70) levels than control mice in diestrus (**Fig. 3*M, N***). Therefore, we can exclude, once again, a PCOS-like reproductive phenotype mediated by the lack of melanocortin signaling.

Kiss1^{ARH} neurons are excited by MC4R agonists

Based on the expression of *Mc4r* in Kiss1 neurons and the reproductive impairment found after *Mc4r* deletion within Kiss1 neurons (**Figure 2**), we hypothesized that Kiss1^{ARH} neurons are direct targets of melanocortins and would respond to MC4R activation. Initially we did whole-cell, voltage clamp recordings in Kiss1^{ARH} neurons (**Figure 4*A***). *Kiss1-Cre* x Ai32 or *Kiss1-Cre* AAV-injected mice underwent ovariectomies (OVX) and were given estradiol (E2) replacement (*see Methods*). We targeted fluorescent cells for recording which were isolated synaptically by bathing the slices in tetrodotoxin (TTX, 1 μM). Focal application of the high-affinity melanocortin receptor agonist melanotan II (MTII, ~250 nM) elicited a small inward current in half of the isolated Kiss1^{ARH} cells (10/21) (**Figure 4*B***). Next, we examined if the E2 state affected MTII response by recording from Kiss1^{ARH} neurons from OVX females and found two thirds (6/9 cells) responded, but there was no significant difference in the average current (**Figure 4*C***). Finally, it must be noted that at this concentration MTII is a non-selective MCR agonist, so we followed up using a perfusion of the MC4R-selective agonist THIQ (100 nM) to determine if activation of MC4Rs alone was sufficient to invoke a postsynaptic response in Kiss1^{ARH} neurons from OVX+E2 females. Similar to MTII, THIQ was able to elicit an excitatory inward current in Kiss1^{ARH} neurons (4/5 cells, -7.4±0.5 pA), indicating MC4R activation is sufficient (**Figure 4*D***).

POMC neurons synapse directly with Kiss1^{ARH} neurons

Based on the pharmacological activation of MCRs, we wanted to address whether POMC^{ARH} neurons are the source of melanocortins to excite Kiss1^{ARH} neurons directly. To answer this question, we injected an AAV-EF1α-DIO-ChR2:mCherry vector into the ARH of adult *Pomc-Cre* female mice (**Figure 4*E***) (24). After 2-4 weeks we did whole cell recordings from putative Kiss1^{ARH} neurons and looked for a response to high frequency optogenetic stimulation of POMC fibers in OVX + E2-treated females (**Figure 4*F***). We were able to confirm that these were Kiss1 neurons based on the presence of a persistent sodium current and/or *post hoc* identification by scRT-PCR (41/69 cells, **Figure 4*G***). While this current is more prevalent in the AVPV Kiss1 population, Kiss1 neurons are the only ARH neurons to display this electrophysiological "fingerprint" of a pronounced INaP paired with a high capacitance and a low input resistance [25]. Additionally, while recording from putative Kiss1^{ARH} neurons, we optogenetically stimulated

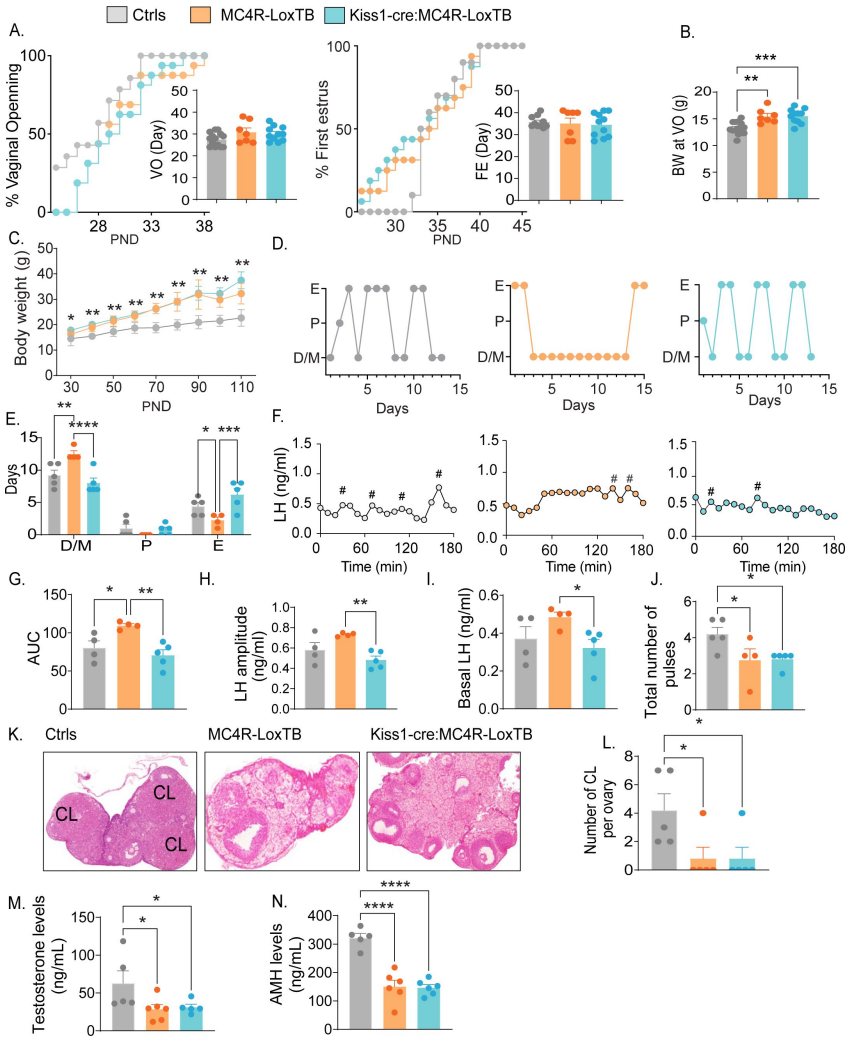

Figure 3.

Re-insertion of MC4R in Kiss1 neurons restores estrous cyclicity and LH pulsatility in Kiss1-cre:MC4R-LoxTB females.

(A) *Kiss1-cre*:MC4R-LoxTB (n=11) and MC4R-loxTB (MC4RKO) (n=7) displayed normal puberty onset as compared to their control littermates (n=14), as documented by cumulative percent and mean age of animals at vaginal opening and first estrus. **(B)** *Kiss1-cre*:MC4R-LoxTB and MC4R-loxTB both had significantly higher body weights at the time of puberty onset compared to their controls. **P < 0.01, *** P < 0.001 by one way ANOVA. **(C)** MC4R-loxTB (n=7) and *Kiss1-cre*:MC4R-LoxTB (n=11) females displayed significantly higher body weight than their littermates (n=10) from post-natal day 30 onwards, *p<0.05 and **P < 0.01. Data presented as the mean± (SEM). **(D)** Representative examples of estrous cycles of MC4R-loxTB (n=4), *Kiss1-cre*:MC4R-LoxTB (n=5) and control littermate mice, (n=4) assessed by daily monitoring of vaginal smears for 15 days. (D/M: diestrus/metestrus, P: proestrus, E: estrus). **(E)** MC4R-loxTB females displayed irregular estrous cycles, presenting longer time in diestrus and shorter time in estrus compared to control females, while *Kiss1-cre*:MC4R-LoxTB females displayed regular estrous cyclicity, similar to controls. *p<0.05, **P < 0.01, *** P < 0.001, ****P < 0.0001, Two-way ANOVA. Data presented as the mean± SEM. **(F)** Pattern of LH pulsatility analyzed in gonad intact MC4R-loxTB (n=4), *Kiss1-cre*:MC4R-LoxTB (n=5) and control littermates females (n=5). LH samples were collected every 10 min for 180 minutes; # represents LH pulses. **(G)** LH total secretory mass, **(H)** LH pulse amplitude, **(I)** basal LH, and **(J)** total number of pulses /180 min were assessed. *p<0.05, **P < 0.01 by one way ANOVA. **(K)** Representative samples of ovarian histology from MC4R-loxTB, *Kiss1-cre*:MC4R-LoxTB and control females (n=5/group); CL: Corpora lutea. Data are presented as the mean± SEM. **(L)** Ovarian histology showed a significant decrease in the number of corpora lutea in the MC4RKO and *Kiss1-cre*:MC4R-LoxTB compared to controls. Groups with different letters are significantly different. Serum levels of **(M)** Testosterone and **(N)** AMH in adult gonad intact females MC4R-loxTB, *Kiss1-cre*:MC4R-LoxTB and their control littermates. *p<0.05, ****P < 0.0001, One Way ANOVA. Data are presented as the mean± SEM.

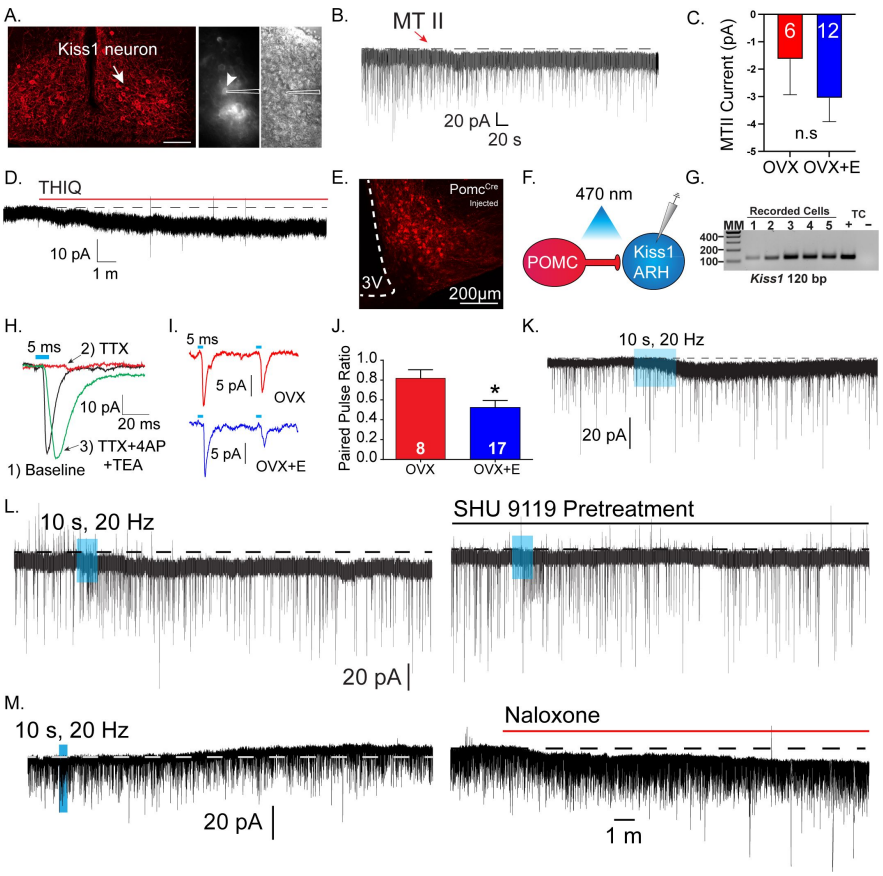

Figure 4.

Kiss1^{ARH} neurons are activated by melanocortin agonists and respond to optogenetic stimulation of POMC neurons.

(A) Slices were taken from *Kiss1-cre* injected (confocal image) brains to target fluorescent cells (arrowhead) for recording (white outline over electrode). **(B)** Whole cell voltage clamp recording of Kiss1^{ARH} neurons following the direct application of the high affinity melanocortin receptor agonist melanotan II (MTII, 250 nM) was added directly to the bath and the response was compared between slices from OVX and OVX+E females. **(C)** While the average inward current was slightly higher in the OVX+E state, this was not a significant difference (Student's t-test for unpaired samples, p>0.05). **(D)** The MC4R-selective agonist THIQ (100 nM) was perfused, and excitatory inward currents were generated in Kiss1^{ARH} neurons. **(E)** Images are of AAV-driven labeling of POMC cells as seen through the confocal. **(F)** Using the AAV-driven expression of channelrhodopsin in adult *Pomc-cre* mice, high frequency stimulation elicited a slow inward current in Kiss1 neurons. **(G)** The identity of cells was confirmed through the presence of a persistent sodium current (see [25]) and/or with RT-PCR of harvested cytoplasm showing *Kiss1* expression. (Gel: MM=molecular marker, TC=tissue controls). **(H)** A direct synaptic projection from POMC to Kiss1^{ARH} neuron (*posthoc* identified) was confirmed using the "rescue" protocol: 1, baseline glutamatergic responses were initially generated (black trace); 2, then action potentials were eliminated by blocking voltage-gated sodium channels with TTX and the postsynaptic response (red trace); 3, blockade of potassium channels facilitated calcium entry into the terminal through ChR2 to release synaptic vesicles, "rescuing" the postsynaptic glutamate response (green trace). **I)** Glutamatergic responses were also often observed, particularly in the ventral ARH. As seen when targeting low input resistance neurons (i.e., Kiss1^{ARH}) with low frequency optogenetic stimulation (5 ms pulse, 50 ms inter-spike interval), the first response in OVX + vehicle females was larger relative to the second response in OVX + E2-treated female mice. Representative traces are the average of 30 sweeps. **(J)** The averaged paired-pulse ratio was lower in recordings from estradiol-treated female mice, indicating an increased release probability (Students t-test p<0.05,). **(K)** High frequency optogenetic stimulation elicited a small inward current. **(L)** In a different cell, a high frequency inward current was noted before constant perfusion of SHU9119 for 15 minutes (break between traces). When the stimulation protocol was repeated, no inward current was elicited. **(M)** The majority of high frequency responses were inward and only twice was an inhibitory outward current recorded in identified Kiss1^{ARH} neurons. Perfusion of the non-selective opioid receptor antagonist naloxone reversed the current, eliminating MCR-activation as the mechanism.

POMC fibers at low frequency (1 Hz, 5 ms, 470 nm light) and recorded fast postsynaptic inward currents. The fast kinetics of the EPSC are also a tell-tale sign of an ionotropic glutamatergic response [26]. Previously, CNQX was sufficient to block similar excitatory ESPCs in other postsynaptic targets of POMC neurons [27]. While the consistent latency from optogenetic stimulus and current response was indicative of a single synaptic delay, we wanted to establish that it was a direct synaptic connection, as we have previously shown for output of POMC neurons [27] and Kiss1 neurons [28–30]. First, we abrogated the optogenetic response with the addition of TTX (1 μM) to the bath, we were able to rescue the postsynaptic glutamate response with the addition of the K^+ channel blockers 4-aminopyridine (4-AP; 0.5 mM) and tetraethyl ammonium (TEA; 7.5 mM) (**Figure 4*H***). K+ channel block enables the calcium influx from ChR2 activation in the presynaptic terminals to be sufficient to restore vesicle fusion. Therefore, there appears to be no intervening synapses between POMC and the downstream $Kiss1^{ARH}$ neurons.

Previously we found that E2 increases glutamate release from POMC neurons by increasing *Vglut2* [27]. Therefore, we compared the postsynaptic glutamatergic responses following two optogenetic stimuli (50 ms interval between light flashes) in $Kiss1^{ARH}$ neurons from OVX + vehicle versus OVX + E2-treated female mice (**Figure 4*I***). As anticipated, we found that treatment with E2 increased the probability of glutamate release from POMC neurons onto $Kiss1^{ARH}$ neurons based on the significant decrease in the paired pulse ratio of the two stimuli [31] (**Figure 4*J***). Although in the present study we used an *in vivo* treatment paradigm, we know from previous studies that this augmentation of glutamate release can happen quite rapidly after a brief exposure to E2 *in vitro* (within 15 min) [27]. Therefore, $Kiss1^{ARH}$ neurons are excited by the glutamatergic input from POMC neurons in an E2-dependent manner.

Finally, given that POMC neurons project directly onto $Kiss1^{ARH}$ neurons, we wanted to show that the evoked slow inward current with high frequency stimulation was mediated by αMSH. Indeed, high frequency stimulation evoked an excitatory inward current (**Figure 4*K***) that was blocked by the selective MC3/4R antagonist SHU 9119 (**Figure 4*L***). The number of high frequency (peptidergic) responses seen in Kiss1 neurons that displayed low frequency postsynaptic (glutamatergic) currents was low (4/16, 25%, mean inward current: -1.4±3.1 pA). However, since these recordings were made in brain slices from E2-treated OVX females and β-endorphin (another product of POMC neurons) expression is enhanced by E2 treatment [32], we were concerned that co-release of this opioid peptide could obscure melanocortin postsynaptic effects. Indeed, there was a notable increase in slow inward currents generated by high frequency stimulation of POMC fibers in slices that were perfused with the non-selective opioid antagonist naloxone (1 μM) (9/23, 40%, mean inward current: -7.6±2.9 pA) (**Figure 4*M***).

Together these optogenetic findings reinforced our pharmacological results showing that $Kiss1^{ARH}$ neurons are excited by MTII, and THIQ. Additional studies would need to be done to identify the cation conductance that is affected by the MC4R signaling cascade in $Kiss1^{ARH}$ neurons, but clearly we have established that there are excitatory glutamatergic and peptidergic inputs from POMC to $Kiss1^{ARH}$ neurons.

$Kiss1^{AVPV/PeN}$ neurons are inhibited by MC4R agonists

Having established a direct, excitatory projection from POMC to $Kiss1^{ARH}$ neurons, we next examined POMC inputs to $Kiss1^{AVPVPeN}$ neurons. First, we used immunocytochemistry to label fibers expressing αMSH to demonstrate that POMC fibers densely innervated the AVPV/PeN area (**Figure 5*A***). Next, we recorded from AVPV neurons in slices taken from OVX+E2, POMC-Cre mice injected with AAV1-DIO-YFP:ChR2 into the ARH (**Figure 5*B***). We targeted cells along the ventricle in the AVPV and PeN, surrounded by YFP terminals, and $Kiss1^{AVPV/PeN}$ neurons were identified based on the expression of several endogenous conductances (I_{NaP}, T-type calcium current, h-current) that are unique to these neurons [25,33]. We recorded a direct glutamatergic synaptic response following optogenetic stimulation in 5 neurons, which was further verified

through pharmacological "rescue" of the synaptic response in 3 out of the 4 neurons tested (**Figure 5C**), indicating that POMC neurons make direct monosynaptic connections with Kiss1$^{AVPV/PeN}$ neurons. We hypothesized that Kiss1$^{AVPV/PeN}$ neurons would be excited by exogenous application of melanocortins because the receptor is typically Gs-coupled [34,35]. We did whole-cell, voltage clamp recordings from Kiss1$^{AVPV/PeN}$-Cre::Ai32 neurons, which were isolated synaptically by bathing the neurons in TTX (1 μM), from OVX females. For these experiments, we tested the response to the high affinity melanocortin receptor agonist MTII (500 nM). Surprisingly, we consistently measured an outward (inhibitory) current that could be reversed on washout of MTII (**Figure 5D**). This outward current was associated with an increase in a K^+ conductance based on the current-voltage plot (*i.e.*, the outward current reversed at ~E_{K+}, **Figure 5E**). Also, the inwardly-rectifying I/V could indicate that MC4R is coupled to activation of inwardly-rectifying K^+ channels as has been previously reported for MC4R signaling in pre-autonomic parasympathetic neurons in the brainstem [36]. We hypothesized that the coupling could be modulated by E2 via a $G\alpha_q$-coupled membrane estrogen receptor (Gq-mER) as we have previously demonstrated in POMC neurons [37–39]. For these experiments, we again utilized OVX females and targeted Kiss1$^{AVPV/PeN}$-Cre::Ai32 neurons. Once in the whole-cell voltage-clamp configuration, we perfused the slices with STX (10 nM), a selective ligand for the putative Gq-mER [39], and tested the response to the MTII. Indeed, the outward current (inhibitory) response to MTII was completely abrogated and even reversed by STX (**Figure 5F, G**). The short-term (bath) treatment with STX ensured that there was no desensitization of the Gq-mER with longer-term (*in vivo*) treatment with E2. Therefore, estrogen receptor activation can rapidly uncouple (*i.e.*, desensitize) the MC4R inhibitory response in Kiss1$^{AVPV/PeN}$ neurons.

We would predict that the intracellular signaling cascade for the heterologous desensitization is similar to what we have elucidated in POMC neurons [39], but this will need to be determined in future experiments. We next investigated the response in vehicle-treated, OVX females. Indeed, Kiss1$^{AVPV/PeN}$ neurons were even more inhibited by the same MTII exposure (**Figure 5G**). Therefore, in contrast to Kiss1^{ARH} neurons, the MC4R appears to be coupled to opening of K^+ channels in Kiss1$^{AVPV/PeN}$ neurons. To further establish whether the MTII was having pre-or postsynaptic effects, we measured the glutamatergic mEPSCs before and after melanocortin receptor activation. We found there was no significant effect on the frequency (**Figure 5H**), but there was an effect on the amplitude (**Figure 5I**). This further supports a postsynaptic locus of STX's effects. However, *posthoc* comparisons found STX increased amplitude compared to both OVX and OVX+E. This result hints at a membrane delimited effect as STX is a much more potent agonist for Gq-mER than E2 [40].

Discussion

Our findings show that melanocortins act directly on Kiss1 neurons to contribute to the metabolic regulation of fertility, in line with previous reports showing that αMSH stimulates LH release in a kisspeptin-dependent manner [13] and that Kiss1 neurons express the melanocortin receptor MC4R [17–20]. Several studies in humans have linked *MC4R* mutations to reproductive abnormalities, including precocious puberty [8], PCOS [9], and hypogonadism [7]. However, a direct association between *MC4R* mutations and reproductive function, independent from the obese condition of these patients, has not been identified [6]. In the current study, we show that the reproductive impairments observed in MC4R deficient mice, which replicate many of the conditions described in humans, are largely mediated by the direct action of melanocortins via MC4R on Kiss1 neurons and not to their obese phenotype. This is because the ablation of MC4R from Kiss1 neurons largely replicated the reproductive impairments observed in MC4RKO female mice without inducing obesity, and the selective reinsertion of MC4R into Kiss1 neurons of MC4RKO mice significantly improved their reproductive function without changing their obese phenotype. Strikingly, puberty onset was advanced in Kiss1-MC4RKO females. Our findings revealed a low melanocortin tone in the hypothalamus of WT females during pubertal

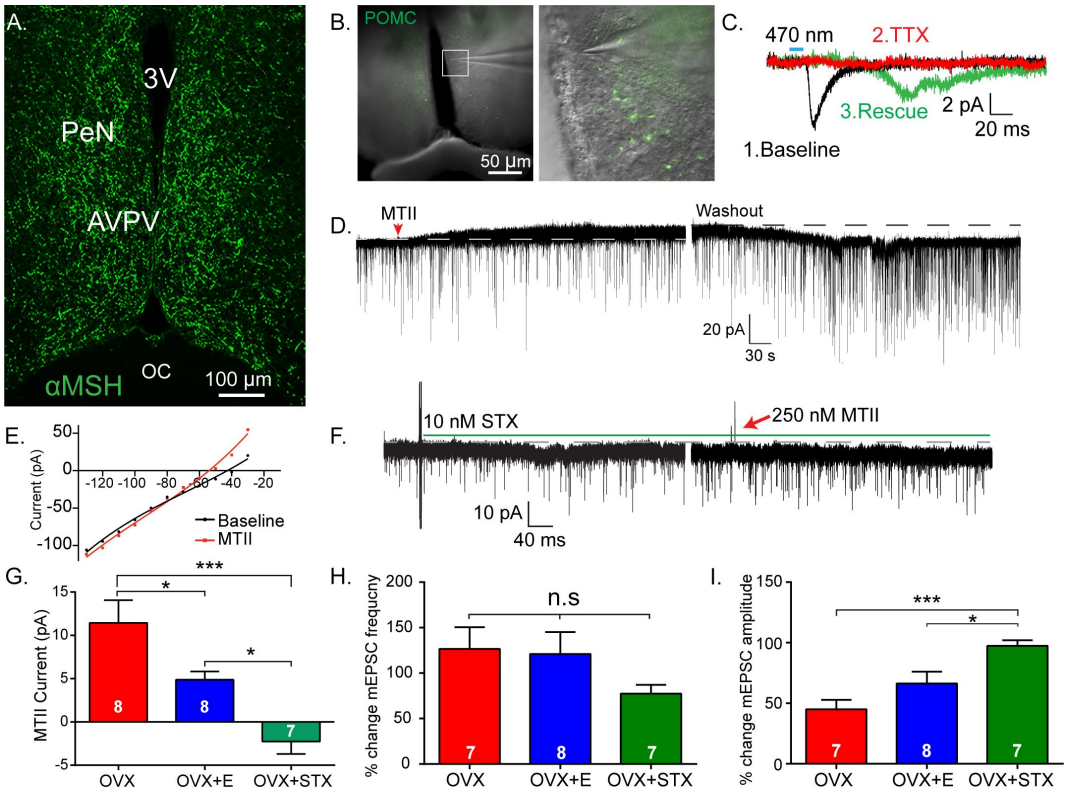

Figure 5.

Kiss1$^{AVPV/PeN}$ neurons are inhibited by MC4R agonists in an E2-dependent manner.

(A) Immunohistochemistry showing robust labeling of α-MSH fibers in the AVPV/PeN region in OVX+E2 WT female mice. **(B)** Low and high power bright-field images taken during electrophysiology recording in OVX+E2 POMC-Cre mice expressing YFP:ChR2 in the ARH following AAV injection. (left) Low power image shows the location of recorded cells. (right) Higher power image of area from white box inset displaying POMC fibers innervating the area. **(C)** Fibers surrounded putative Kiss1-AVPV neurons (expressing I_{NaP}, IT and I_h) and optogenetic stimuli was able to elicit postsynaptic currents that were eliminated with tetrodotoxin (1 µM), but "rescued" with addition of K^+ channel blockers (4-AP and TEA) which indicates a monosynaptic connection between POMC^{ARH} and Kiss1^{AVPV} neurons. **(D)** Whole-cell voltage clamp recordings were made in ChR2-YFP positive cells in brain slices taken from *Kiss1-cre*:Ai32 female mice. Bath application of melanotan II (MTII, 500 nM) generated an inhibitory outward current in a Kiss1$^{AVPV/PeN}$ neuron from OVX female. As the cell was synaptically isolated using bath-applied tetrodotoxin (TTX, 1 µM) this represents a direct effect. Washout of MTII while still in TTX quickly led to a return to baseline RMP. **(E)** An IV relationship was plotted using voltage steps before and after MTII administration. The crossing at -80 mV (~EK^+) indicates that the opening of K+ channels underlie the MC4R inhibition of Kiss1^{AVPV} neurons. **(F)** In a subset of recordings from OVX brains slices, the selective membrane estrogen receptor (Gq-mER) agonist STX (10 nM) was added to the bath for ~10 minutes prior to addition of MTII. STX pretreatment resulted in either a greatly attenuated outward current or even an inward current as shown in this example. **(G)** The mean outward current was significantly higher when recording in Kiss1$^{AVPV/Pen}$ neurons from brain slices from vehicle-treated, OVX females compared to E2-treated, OVX females or acute STX-treated brain slices from OVX females (One-way ANOVA $F_{(2,19)}$=12.32, p<0.001; Holm-Sidak *posthoc* comparisons found significant differences between all groups; * p<0.05, *** p<0.001). **(H)** There was no difference in the frequency of mEPSCs after MTII, calculated as a percent of baseline between groups. **(I)** However, there was a significant difference in the mEPSC amplitude (calculated as a percent of baseline) between all groups: main effect $F_{(2,19)}$ =10.58, p<0.001. *Posthoc* comparisons using Holm-Sidak found OVX+STX to be different from both OVX (p<0.001) and OVX+E (p<0.05).

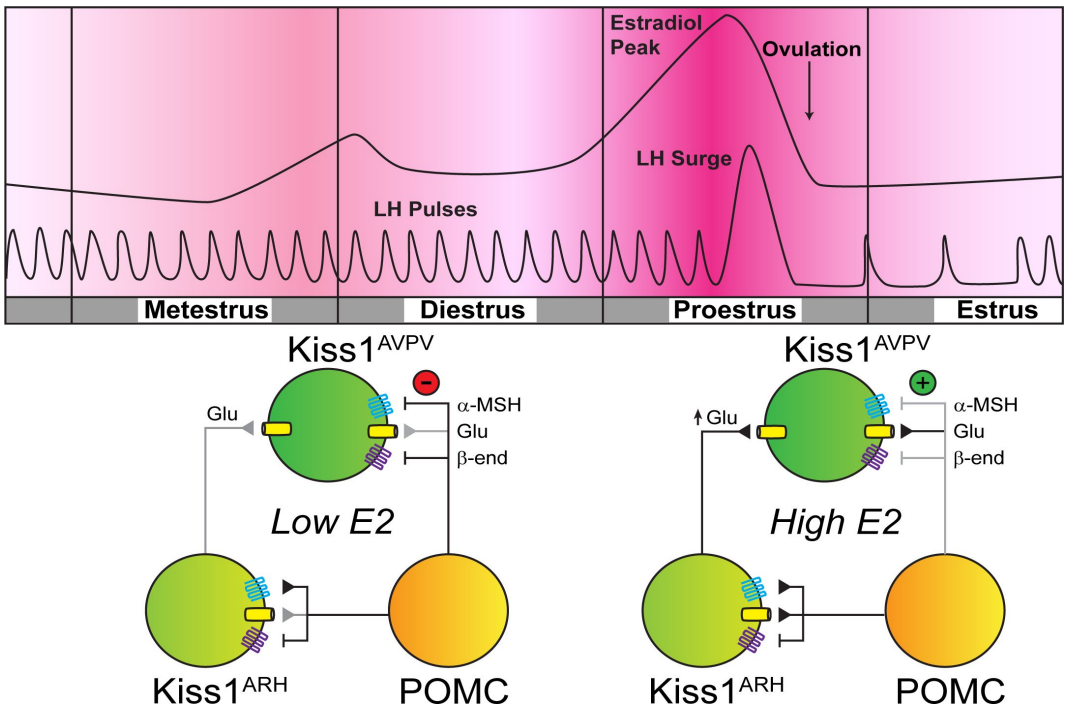

Figure 5. (continued)

development, characterized by lower levels of *Agrp, Mc4r* and *Mc3r* expression at the time of puberty onset (~PND30). This developmental decline in the expression of melanocortin receptors is in line with the advanced timing of puberty onset in females when MC4R is congenitally ablated from Kiss1 neurons. A recent study using whole body MC3RKO mice showed a trend to delayed puberty onset [18], suggesting a larger role of melanocortins in the timing of puberty onset. Here, we show that in females the combination of MC3R and MC4R action may be necessary for pubertal development. Interestingly, the MC4R-LoxTB and *Kiss1-cre:MC4R-LoxTB* mice do not show an advancement in puberty onset as we observed in Kiss1-MC4RKO mice; however, these mice are obese at the time of puberty onset already, which may affect the timing of sexual maturation independently of MC4R action in Kiss1 neurons. Of note, the findings presented in this study do not rule out the existence of additional sites of action of MC4R in other neuronal populations to regulate reproduction, *e.g.,* GnRH neurons, which also express MC4R [15,24]. Indeed, the lack of full recovery of the reproductive function in *Kiss1-cre:MC4R-LoxTB* mice suggests that MC4R in Kiss1 neurons is necessary but not sufficient to achieve full reproductive capabilities.

In addition to early puberty onset, Kiss1-MC4RKO females displayed an impaired preovulatory LH surge driving ovulation and had fewer corpora lutea in their ovaries compared to control littermates, further supporting a role of MC4R in regulating ovulation. In adulthood, the reproductive phenotype observed in Kiss1-MC4RKO and MC4R-loxTB female mice (increased LH, irregular estrous cycles, oligo-ovulation, increased cystic follicles) correlates with the phenotype observed in PCOS mouse models [21,22]. In fact, an association between *MC4R* mutations and PCOS has been reported [9]. However, our mouse models failed to display higher levels of circulating androgens or AMH, two of the hallmarks of PCOS [23], suggesting that melanocortin signaling is unlikely to be a main contributing factor in the development of this syndrome.

Our data revealing early puberty onset and impaired LH pulse and surge driving ovulation support a direct role of MC4R on the two primary Kiss1 populations regulating these functions (ARH and AVPV/PeN). We further investigated this and found that MC4R signaling excites $Kiss1^{ARH}$ neurons and inhibits $Kiss1^{AVPV/PeN}$ neurons in an estradiol-dependent manner. In $Kiss1^{ARH}$ neurons, bath applied or optogenetically-evoked release of melanocortin agonists induce a direct excitatory inward current. Our studies using whole cell voltage clamp in female mice were able to detect a melanocortin-mediated inward current in $Kiss1^{ARH}$ neurons that would increase excitability. Previously, an MCR-activation effect was not detected in cell-attached recordings of diestrus females [13]. However, cell-attached recordings do not measure a direct response in isolated $Kiss1^{ARH}$ neurons but rather the summation of multiple synaptic inputs to $Kiss1^{ARH}$ neurons. Most importantly, we did not see a difference in the excitatory response in synaptically isolated $Kiss1^{ARH}$ neurons from E2-treated versus vehicle-treated, ovariectomized females. This emphasizes the importance of doing whole-cell recording from isolated Kiss1 neurons. The modulatory actions of $POMC^{ARH}$ neuronal projections to $Kiss1^{ARH}$ neurons can also occur through a) the excitatory action of glutamate in a process that is facilitated in the presence of estradiol, in line with previous publications [41,42], and b) the inhibitory action of β-endorphin, suggesting that $POMC^{ARH}$ neurons are able to exert a precise regulatory role of the GnRH pulse generator, *i.e.* $Kiss1^{ARH}$ neurons, in response to metabolic challenges. In the AVPV/PeN, MC4R agonists inhibited $Kiss1^{AVPV/PeN}$ neurons in an estradiol-dependent manner, which utilized a $G\alpha_q$-coupled membrane estrogen receptor (STX receptor) to attenuate the inhibitory tone of MC4R in these neurons.

Our pharmacology data clearly demonstrates the estradiol-dependent action of MC4R in $Kiss1^{AVPV/PeN}$ neurons, suggesting that similar to $Kiss1^{ARH}$ neurons, this population is tightly controlled by melanocortins. The effect of MC4R agonists on Kiss1 neurons in the presence of TTX, suggests a direct synaptic effect without the need of channelrhodopsin-2(ChR2)-assisted circuit mapping. Nonetheless, to further demonstrate this interaction, we provide evidence of profound innervation of αMSH fibers and the presence of synaptic contact between POMC and $Kiss1^{AVPV/PeN}$ neurons through the optogenetic stimulation of a glutamatergic response in $Kiss1^{AVPV/PeN}$ neurons

after low frequency stimulation of POMC terminals. We intentionally avoided high frequency stimulation of POMC terminals to prevent the co-release of β-endorphins (e.g., **Figure 4M**) and their possible additive effect on the inhibitory action of MC4R. Future studies will be aimed at the characterization of the endogenous opioid pathways in the induction of the LH surge.

To date, two instances of MC4R-mediated inhibition have been described in the central nervous system: MC4R can Gi,o couple to open K+ (Kir6.2) channels in parasympathetic preganglionic neurons in the brainstem [36], and MC4R can directly couple to K+ (Kv7.1) channels in the hypothalamic paraventricular nucleus neurons [43]. Interestingly, our findings describe an inhibitory role of MC4R in the reproductive neuroendocrine axis. This steroid state dependent effect is particularly relevant because in the context of reproduction, the two populations of Kiss1 neurons are strikingly different in their response to estradiol, where peptide expression in $Kiss1^{ARH}$ and $Kiss1^{AVPV/PeN}$ neurons are inhibited or stimulated, respectively, in order to mount the negative versus positive feedback of sex steroids [14]. This differential regulation allows for the episodic versus surge release of GnRH; however, the cellular mechanisms underlying these opposing roles of Kiss1 neurons to the same stimulus, *i.e.* circulating E2 levels, remain unknown. Although there were no differences in the magnitude of the electrophysiological responses to MTII in $Kiss1^{ARH}$ neurons in vehicle-versus E2-treated, ovariectomized females, we cannot rule out that E2 affects other systems activated by the MC4R signaling cascade as recently reported in MC4R expressing neurons of the ventromedial nucleus of the hypothalamus (VMH) [44]. Interestingly, puberty onset was advanced in Kiss1-MC4RKO females. This data suggests that the inhibitory tone of MC4R signaling on $Kiss1^{AVPV/PeN}$ neurons might also be involved in the timing of puberty onset, which in turn suggests a role for this female-specific population of Kiss1 neurons in sexual maturation. This phenomenon could explain the earlier age of puberty onset frequently seen in females of most mammalian species compared to their male counterparts [45]. Furthermore, our findings suggest that metabolic cues, through the regulation of the melanocortin output onto $Kiss1^{AVPV/PeN}$ neurons, are essential for the timing and magnitude of the GnRH/LH surge. Future studies are warranted to fully elucidate synaptic input and postsynaptic cascades in the POMC-$Kiss1^{AVPV/PeN}$ circuit.

Altogether, our data reveal a differential regulatory action of MC4R in the neural control of GnRH/LH release, participating in both the surge (E2-treated, ovariectomized female) and the pulse-like (ovariectomized female) modes of LH release through the cellular regulation of Kiss1 neurons, which translate into our findings on the conditional knockout of *Mc4r* from Kiss1 neurons (**Figure 6**). These findings are important because the reproductive abnormalities often attributed to obesity in MC4R deficient patients may not be caused by the excess in body weight but, at least in part, by a deficiency in MC4R signaling directly at the level of Kiss1 neurons that affects predominantly the ability to mount a preovulatory LH surge.

Materials and methods

In-vivo experimental procedures

Generation of Kiss1-MC4RKO, Kiss1-cre:MC4R-LoxTB and MC4R-LoxTB Transgenic Mice

Kiss1-MC4RKO mice were generated by crossing *Kiss1-cre* knock-in mice and $MC4R^{lox/lox}$ mice. *Kiss1-cre* mice (RRID:MGI:6278139) were obtained from Dr. Richard Palmiter (University of Washington, Seattle, WA) [46] and $Mc4r^{lox/lox}$ (RRID:IMSR_JAX:023720) were a gift from Dr. Brad Lowell (Beth Israel Deaconess Hospital, Boston, MA) [4]. These mice were crossed to generate Kiss1-MC4RKO mice lacking *Mc4r* expression selectively from Kiss1 neurons ($Kiss1\text{-}cre^{+/-}$; $MC4R^{lox/lox}$) and their control littermates ($MC4R^{lox/lox}$). To generate *Kiss1-cre:MC4R-LoxTB* and

MC4R-LoxTB mice, *MC4R-LoxTB* mice were purchased from The Jackson Laboratory (MC4R-LoxTB; catalog no. 006414). These mice present with a loxp-flanked transcriptional blocking (LoxTB) sequence preventing normal endogenous gene transcription and translation from the endogenous locus. Homozygous MC4R-loxTB/loxTB mice are devoid of functional MC4R mRNA (MC4RKO mice), while the presence of Cre recombinase on the Kiss1 promotor in *Kiss1-cre* mice will result in the removal of the transcription blocker and subsequent expression of MC4R in tissue-specific sites (*i.e.* Kiss1 neurons) therefore resulting in the generation of *Kiss1-cre*:MC4R-LoxTB (with *Mc4r* expression restored in Kiss1 neurons), their obese control littermates *MC4R-LoxTB* mice (MC4RKO), and their WT controls ($MC4R^{+/+}$). To rule out early embryonic recombination of the $MC4R^{loxTB/loxTB}$ or $MC4R^{lox/lox}$ alleles, we ran PCR assays on tail DNA designed to detect wild-type allele ($MC4R^{+/+}$), undeleted lox ($MC4R^{lox/lox}$) or loxTB alleles ($MC4R^{loxTB/loxTB}$). Genotyping was confirmed by sending tissue to Transnetyx, Inc., for testing by real-time polymerase chain reaction. Mice were housed in Harvard Medical School Animal Resources facilities where they were fed standard mouse chow (Teklad F6 Rodent Diet 8664) and were given *ad libitum* access to tap water under constant conditions of temperature (22–24°C) and light (12 hr light [07:00]/dark [19:00] cycle).

RNAscope in situ hybridization

To validate the Kiss1-MC4RKO, *Kiss1-cre*:MC4R-LoxTB and MC4R-LoxTB (MC4RKO) mouse models and investigate the co-expression of *Kiss1* and *Mc4r* mRNA in these mice, dual fluorescence ISH was performed using RNAscope (ACD, Multiplex Fluorescent v.2) according to the manufacturer's protocol using the following probes: *Mc4r* (319181-C2) and *Kiss1* (500141-C1). Brains (n=4/group) from WT OVX (for expression in the ARH) and OVX+E2 (for expression in the AVPV/PeN) mice and OVX Kiss1-MC4RKO, *Kiss1-cre*:MC4R-LoxTB and MC4RKO were removed fresh frozen on dry ice, and then stored at -80°C until sectioned. Five sets of 20 µm sections in the coronal plane were cut on a cryostat, from the diagonal band of Broca to the mammillary bodies, thaw mounted onto SuperFrost Plus slides (VWR Scientific) and stored at -80°C until use. A single set was used for ISH experiment (adjacent sections 100 mm apart). Images were taken at 20x magnification of the sections containing AVPV, PeN, and the three rostro-to-caudal levels of the ARH, and Kiss1 neurons expressing (*Kiss1-cre*:MC4R-LoxTB mice) or lacking (Kiss1-MC4RKO mice) *Mc4r* were identified using ImageJ.

Reproductive maturation of Kiss1-MC4RKO, *Kiss1-cre*:MC4R-LoxTB and MC4R-LoxTB mice

To assess the reproductive phenotype of mice with selective reinsertion of *Mc4r* on Kiss1 neurons (*Kiss1-cre*:MC4R-LoxTB, n=11), selective deletion of *Mc4r* from Kiss1 neurons (Kiss1-MC4RKO, n=24), global deletion of *Mc4r* (MC4R-LoxTB, n=7); and their control $MC4R^{lox/lox}$ littermates (n=14), mice were weaned at post-natal day (PND) 21 and were monitored daily for puberty onset. Females were monitored daily for vaginal opening (VO, indicative of the complete canalization of the vaginal cavity) and for first estrus (first day with cornified cells determined by daily morning vaginal cytology) after the day of VO. Body weight (BW) was measured at the day of puberty onset to determine if changes in puberty onset could be due to differences in BW. Estrous cyclicity was monitored in females by daily vaginal cytology, for a period of 15 days, in 6-month-old mice and their respective control littermates (n=5/group). Cytology samples were obtained every morning (9 am), placed on a glass slide and stained with hematoxylin and eosin for determination of the estrous cycle stage under the microscope.

Fecundity test of Kiss1-MC4RKO females

Adult 6-month-old Kiss1-MC4RKO and control littermate female mice (n=9/group) were placed with adult WT males proven to father litters for 90 days and time to deliver pups and number of pups per litter were monitored.

Characterization of the estradiol-induced luteinizing hormone surge

Kiss1-MC4RKO (n=6) and control MC4R$^{lox/lox}$ littermate (n=5) adult female mice were subjected to bilateral ovariectomy (OVX) via abdominal incision under light isoflurane anesthesia. Immediately after OVX, capsules filled with E2 (1 ug/20g BW) were implanted subcutaneously via a small mid-scapular incision on the back. Five days later, mice were subcutaneously injected in the morning with estradiol benzoate (1 ug/20g BW) to produce elevated proestrus-like E2 levels (preovulatory LH surge) on the following day [47]. Blood samples were collected at 8am and 7pm; LH levels were stored at -80°C until measured via LH ELISA.

Ovarian histology and hormone measurements

Bilateral ovariectomy from 6-month-old Kiss1-MC4RKO (n=4), *Kiss1-cre*:MC4R-LoxTB, MC4R-LoxTB and their control littermates (n=5/group) was performed under light isoflurane anesthesia. Briefly, the ventral skin was shaved and cleaned, and one small abdominal incision was made. Once the ovaries were identified and excised, the muscle incision was sutured, and the skin was closed with surgical clips. Ovaries were stored in Bouin's fixative, sectioned, and stained with hematoxylin and eosin at the Harvard Histopathology Core. Corporal lutea were counted in the middle section of each ovary. Serum samples were also collected for analysis of testosterone and anti-müllerian hormone (AMH) levels in these mice. These hormones levels were measured at the University of Virginia Ligand Assay core with the Mouse & Rat Testosterone ELISA assay (reportable average range 10-1600 ng/dL; sensitivity of 10 ng/dL); AMH ELISA assay (reportable average range 0.2 – 15 ng/mL; sensitivity of 0.2 ng/mL).

LH pulsatile secretion profile in gonad intact Kiss1-MC4RKO, *Kiss1-cre*:MC4R-LoxTB and MC4R-LoxTB female mice

To assess the profile of LH pulses secretion, adult 6 months old gonad intact Kiss1-MC4RKO females (n=6), their control Mc4r$^{lox/lox}$ littermates (n=7); and *Kiss1-cre*:MC4R-LoxTB (n=5/group), MC4R-LoxTB and their control WT females (n=4/group) were handled daily for 3 weeks to allow acclimation to sampling conditions prior to the experiment. Pulsatile measurements of LH secretion were assessed by repeated blood collection through a single incision at the tip of the tail. The tail was cleaned with saline and 4 µL of blood was taken at each time point from the cut tail with a pipette. We collected sequential blood samples every 10 minutes over a 180-minute sampling period. Samples were immediately frozen on dry ice and stored at −80 °C until analyzed with LH ELISA as previously described [48]. The functional sensitivity of the ELISA assay was 0.0039 ng/ml with a CV% of 3.3%.

LH pulses analysis

LH pulses in mice were analyzed using a custom-made MATLAB-based algorithm. The MATLAB code includes a loop that determines LH pulses as any LH peak: (i) whose height is 20% greater than the heights of the 2 previous values; (ii) 10% greater than the height of the following value; and (iii) the peak at the second time interval needs to be 20% greater than the single value that comes before it to be considered a pulse, as we previously described [49].

LH pulsatility was assessed by measuring: (1) the total secretory mass, assessed by area under the curve (AUC); (2) the LH pulse amplitude, calculated by averaging the 4 highest LH values in the samples collection period for each animal; (3) the basal LH, calculated by averaging the 4 lowest LH values in the samples collection period for each animal; and (4) the total number of pulses throughout the 180 minutes sampling period.

Immunohistochemistry

Animals and Treatment

Coronal brain blocks (2 mm each) from adult female C57BL/6 mice (n=4) were fixed by immersion in 4% paraformaldehyde for ~ 8 hours, cryoprotected in 30% sucrose solution, frozen in isopentane at –55°C, sectioned coronally on a cryostat at 20 µm, and thaw-mounted onto Superfrost Plus slides (Fisher Scientific, Pittsburgh, PA). The 20 µm sections were stored at –20°C until used for immunocytochemistry.

Immunocytochemistry

The sections were rinsed in PB (0.1M phosphate buffer, pH 7.4) for at least 30 min. Next, sections were incubated with normal serum corresponding to the host for the secondary antiserum (5 % normal serum with 0.3% Triton-X100 in PBS for 30 min), rinsed in PB and then incubated for ~45 h at 4° C with a rabbit polyclonal antiserum against α-MSH (1:2,500). The specificity of this antiserum has been documented [50]. After rinsing, sections were first incubated for 2-3 hours at room temperature with biotinylated donkey anti rabbit gamma globulin (IgG; 1:500) and next with streptavidin-Alexa 488 (1:2500). Both the primary and secondary antibodies were diluted in tris-(hydroxymethyl) aminomethane (0.5 %, Jackson ImmunoResearch, Philadelphia, PA) in PB containing 0.7 % seaweed gelatin (Jackson ImmunoResearch, Philadelphia, PA) and 0.5 % Triton X-100 and 3% bovine serum albumin (BSA; Jackson ImmunoResearch, Philadelphia, PA) adjusted to pH 7.6. Following a final rinse overnight, slides were coverslipped with gelvatol containing the anti-fading agent, 1,4-diazabicyclo(2,2)octane (DABCO; Cold Spring Harbor Protocols, 2006).

Imaging

Photomicrographs of labeling were initially acquired using a Nikon E800 fluorescent microscope (Eclipse E800; Nikon Instruments, Melville, NY) equipped with a fiber illuminator (Intensilight C-HGFI; Nikon Instruments) and a high-definition digital microscope camera head (DS-Fi1; Nikon Instruments) interfaced with a PC-based camera controller (DS-U3; Nikon Instruments).

Real time quantitative PCR

i) To investigate the changes in the expression of the melanocortin genes *Agrp*, *Pomc*, *Mc3r* and *Mc4r* in the MBH during development in prepubertal and pubertal WT females at ages P10 (n=6), P15 (n=6), P22 (n=6), and P30 (n=5), and ii) evaluate the gene expression profile of *Pdyn*, *Kiss1*, *Tac2*, *Tacr3*, in the ARH of adult intact (in diestrus) female Kiss1-MC4RKO (n=6) and their control $MC4R^{lox/lox}$ littermates (n=3), the brains were removed and rapidly embedded in Tissue-Tek, frozen in −30°C isopentane solution and stored at −80°C until use. Frozen tissue punches were recovered through MBH with a 1 mm diameter canula [51]. These tissue punches encompassed the whole MBH from the WT females and the ARH from the Kiss1-MC4RKO and their control females. The tissues were homogenized, and total RNA was isolated using TRIzol reagent (Invitrogen) followed by chloroform/isopropanol extraction. RNA purity and concentration were measured via an absorbance spectrophotometer (260/280 nm > 1.8; NanoDrop 1000, Thermo Fisher Scientific). Total RNA (1 µg) was reverse transcribed to cDNA using random hexamers (High-Capacity cDNA Synthesis Kit, Life Technologies). Quantitative real-time PCR assays were performed using SYBR Green RT-qPCR master mix (Applied Biosystems) and analyzed using ABI Prism 7000 SDS software (Applied Biosystems). The cycling conditions were: 2 minutes incubation at 95°C (hot start), 45 amplification cycles (95°C for 30 seconds, 60°C for 30 seconds, and 45 seconds at 75°C, with fluorescence detection at the end of each cycle), followed by melting curve of the amplified products obtained by ramped increase of the temperature from 55°C to 95°C to confirm the presence of single amplification product per reaction. PCR specificity was verified by melting curve analysis and agarose gel electrophoresis. Each sample was run in duplicate to obtain an

average cycle threshold (CT) value and relative expression of each target gene was determined using the comparative Ct method [52]. The data were normalized to Hypoxanthine Guanine Phosphoribosyltransferase (*Hprt)* expression levels in each sample. Results were expressed as fold differences in relative gene expression with respect to i) P10 for melanocortin genes expression analysis during development in WT mice, and ii) controls for the KNDy genes expression in female Kiss1-MC4RKO mice. The primers used are listed in Table 1.

Gene	Gene length (pb)	Accession #	Primers	Location (nt)	Sequence
Hprt	352	NM_013556.2	Hprt-F	704-728	CCTGCTGGATTACATTAAAGCGCTG
			Hprt-R	377-401	GTCAAGGGCATATCCAACAACAAAC
Agrp	136	NM_001271806.1	Agrp-F	466-488	GCCTCAAGAAGACAACTGCAGAC
			Agrp-R	580-601	AAGCAGGACTCGTGCAGCCTTA
Pomc	138	NM_001278584.1	Pomc-F	187-208	CCATAGATGTGTGGAGCTGGTG
			Pomc-R	303-324	CACCTCCGTTGCCAGGAAACAC
Mc4r	101	NM_016977.4	Mc4r-F	552-570	CCCGGACGGAGGATGCTAT
			Mc4r-R	632-652	TCGCCACGATCACTAGAATGT
Pdyn	200	NM_018863.4	Pdyn-F	45-64	ACAGGGGGAGACTCTCATCT
			Pdyn-R	223-244	GGGGATGAATGACCTGCTTACT
Kiss1	129	AF472576.1	Kiss1-F	147-166	GCTGCTGCTTCTCCTCTGTG
			Kiss1-R	256-275	TCTGCATACCGCGATTCCTT
Tac2	234	NM_001199971.1	Tac2- F	238-257	GCTCCACAGCTTTGTCCTTC
			Tac2- R	452-471	GCTAGCCTTGCTCAGCACTT
Tacr3	159	NM_021382.6	Tacr3-F	759-779	GCCATTGCAGTGGACAGGTAT
			Tacr3-R	898-917	ACGGCCTGGCATGACTTTTA

Data analysis

Statistical data are expressed as means ± SEM, where n represents the number of animals in each study group. The significance of differences between groups was evaluated using unpaired two-tailed Student's t test, or a one-or two-way ANOVA test (with *post hoc* comparisons). Significance level was set at $p<0.05$. All analyses were performed with GraphPad Prism Software, Inc (San Diego, CA).

In-vitro experimental procedures

Animals

All animal procedures described in the electrophysiology studies were performed in accordance with institutional guidelines based on National Institutes of Health standards and approved by the Institutional Animal Care and Use Committees at Oregon Health and Science University and Appalachian State University. *Pomc-Cre* mice (RRID:IMSR_JAX:005965) [53] were crossed with wildtype C57B6J (RRID:IMSR_JAX:000664) mice. *Kiss1-cre*(v2) mice [46] were crossed with Ai32

[54] or C57B6J mice. All colonies were maintained onsite under controlled temperature (21-23 °C) and photoperiod (12:12-h light-dark cycle 0600 to 1800) while receiving ad libitum food (5L0D; LabDiet, St. Louis, MO) and water access. Following surgeries, mice received a *s.c.* dose of 4-5 mg/kg carprofen (Rimadyl; Pfizer Animal Health, New York, NY) and given at least 1 week of recovery.

Ovariectomies

At least 7 days prior to each experiment, ovaries were removed as described previously while under isoflurane anesthesia [42]. Two days before experiments females received either an injection of sesame oil (50 µl, *sc*; Sigma-Aldrich, St. Louis, MO) or a priming dose (0.25 µg /50 µl sesame oil, *sc*) of E2 benzoate (Sigma-Aldrich, St. Louis, MO) in the morning. On the following day, oil or a high (1.5 µg) dose of E2 benzoate, which generates a LH surge, was administered [55]. Circulating levels of E2 were verified by the uterine weights (<25 mg for OVX and >95 mg for OVX E2-treated) at the time of euthanasia [55].

AAV Delivery

Bilateral ARH injections of AAV1-Ef1a-DIO-ChR2:mCherry (RRID:Addgene_20297) or AAV1-Ef1a-DIO-ChR2:YFP (RRID:Addgene_20298) were performed on adult *Kiss1-cre* mice or *Pomc-cre* mice on a stereotaxic frame under isoflurane anesthesia. ARH injection coordinates were anteroposterior (AP): −1.10 mm, mediolateral (ML): ± 0.30 mm, dorsoventral (DL): −5.80 mm (surface of brain z = 0.0 mm); 400 nl of the AAV (2.0 x 10^{12} particles/ml) was injected (100 nl/min) into each position. Mice were given carprofen for analgesia and allowed to recover for at least two weeks before euthanasia.

Visualized whole-cell patch recordings

Hypothalamic coronal brain slices (240 um) were made from female mice, using a Leica VT1000S vibratome, in ice cold cutting solution bubbled with $O_2/C0_2$ (95%/5%). Slices were then transferred to a holding chamber with artificial cerebrospinal fluid bubbled with the same gas mix and allowed to recover for at least 1 hour. For recordings, slices were placed in a perfusion chamber and visualized with a Olympus BX51W1 using either differential infrared contrast or oblique illumination. Kiss1 neurons in the ARH or AVPV/PeN were targeted for electrophysiological recordings as done previously and described below [56,57].

Solutions/drugs

Standard vibratome slicing, external, and internal recording solutions were utilized as previously described [56,57]. Tetrodotoxin was purchased from Alomone Labs (Jerusalem, Israel), Melanotan II and αMSH from Tocris (Minneapolis, MN). TEA, 4-AP, 17β-estradiol benzoate, and Naloxone were purchased from Millipore-Sigma. STX was produced by AAPharmaSyn, LLC (Ann Arbor, MI) under contract.

Electrophysiology data analysis

Electrophysiological data were analyzed using Clampfit 10/11 (Molecular Devices) and Prism 7/10 (Dotmatics). All values are expressed as Mean ± SEM. Comparisons between two groups were made using un-paired Student's t-test or between multiple groups using an ANOVA (with *post hoc* comparisons) with p-values < 0.05 considered significant. When variances differed significantly, Mann-Whitney U test was used instead.

Targeting of Kiss1 neurons for electrophysiological recordings

For non-optogenetic experiments, brain slices were taken from AAV injected Kiss1-Cre AAV or Kiss1xAi32 female mice. Ai32 mice (RRID:IMSR_JAX:024109, C57BL/6 background) carry the floxed ChR2 (H134R)-EYFP gene in their Gt(ROSA)26Sor Locus [54], allowing its expression in a Cre-

dependent manner. Due to concerns of nonspecific expression [58], we previously validated this model using single cell RT-PCR and documented that *Kiss1* mRNA was detectable in 99% of individually harvested eYFP cells (n=126). In addition, we have used both AAV injected Kiss1-Cre AAV or Kiss1xAi32 female mice and found no differences in electrophysiological results [56]. We used AAV injected POMC-Cre female mice and avoided small soma, high input resistance (>800 MΩ), ventrally located cells that are typically NPY/AgRP neurons. Instead, we targeted larger, more dorsomedial neurons in the ARH while avoiding fluorescent (POMC) cells. Unlike ARH Kiss1 neurons, POMC neurons do not make reciprocal projections, so uninfected POMC neurons do not display monosynaptic EPSCs in response to optogenetic stimulation. Next, we used a ramp IV protocol to probe for the presence of a persistent sodium current (I_{NaP}). While this current is more prevalent in the AVPV Kiss1 population, Kiss1 neurons are the only ARH neurons to display this electrophysiological "fingerprint" of a pronounced I_{NaP} paired with a high capacitance and low input resistance [25]. Finally, we also harvested the cytosol at the end of all recordings and measured the expression of Kiss1. Only cells that expressed a persistent sodium current and/or expressed *Kiss1* mRNA were included in final analysis (n = 44).

Acknowledgements

The authors would like to recognize the excellent technical expertise of Ms. Martha A. Bosch (tissue preparation, immunohistochemical procedure and single cell RT-PCR of recorded neurons). In addition, we thank Dr. Rona Carroll for her assistance at Harvard Medical School and Mr. Cole Martinson, a student worker in the Ronnekleiv/ Kelly laboratories, for his assistance with genotyping and care of mouse colonies at OHSU. The University of Virginia Center for Research in Reproduction Ligand Assay and Analysis Core is supported by the Eunice Kennedy Shriver NICHD/NIH (NCTRI) Grant P50-HD28934. This work was supported by PHS MPI grant DK68098 to MJK and OKR; HD090151, HD099084 and DK133760 to VMN, and The Charles A. King Trust Postdoctoral Research Fellowship Award, The Lalor Foundation Postdoctoral Fellowship Award, the Women's brain initiative Fellowship Award, the ROSA SCORE pilot grant (supported by NIH Research Grant U54 AG062322 funded by The National Institute on Aging (NIA) and Office of Research on Women's Health (ORWH)) and the IBRO-ISN Research Fellowship Award to RT, and startup funds from Appalachian State University to TLS.

Authors contribution

RT, TLS, MJK and VMN conceived and designed the study; RT, TLS, KF, CJH, EM, AG, KW, SL, EAM, OKR performed the experiments. RT, TLS, OKR, MJK and VMN analyzed data. RT, TLS and VMN wrote the manuscript with input from all the authors.

Declaration of interests

The authors declare they have no competing interest.

References

1. Health U. (2020) **Health, U. (2020). Infertility. http://obgyn.ucla.edu/infertility**

2. Andermann M.L., Lowell B.B (2017) **Toward a Wiring Diagram Understanding of Appetite Control** *Neuron* **95**:757–778 https://doi.org/10.1016/j.neuron.2017.06.014

3. Cone R.D (2006) **Studies on the physiological functions of the melanocortin system** *Endocr Rev* **27**:736–749 https://doi.org/10.1210/er.2006-0034

4. Shah B.P., Vong L., Olson D.P., Koda S., Krashes M.J., Ye C., Yang Z., Fuller P.M., Elmquist J.K., Lowell B.B (2014) **MC4R-expressing glutamatergic neurons in the paraventricular hypothalamus regulate feeding and are synaptically connected to the parabrachial nucleus** *Proceedings of the National Academy of Sciences of the United States of America* **111**:13193–13198 https://doi.org/10.1073/pnas.1407843111

5. Wang K., Mao W., Zhang X., Zhao Y., Fan K., Pan D., Liu H., Li P., Hai R., Du C (2020) **Neuroanatomy of melanocortin-4 receptor pathway in the mouse brain** *Open Life Sci* **15**:580–587 https://doi.org/10.1515/biol-2020-0063

6. Farooqi I.S., Keogh J.M., Yeo G.S., Lank E.J., Cheetham T., O'Rahilly S (2003) **Clinical spectrum of obesity and mutations in the melanocortin 4 receptor gene** *The New England journal of medicine* **348**:1085–1095 https://doi.org/10.1056/NEJMoa022050

7. Hainerová I.A., Zamrazilová H., Sedláčková D., Hainer V (2011) **Hypogonadotropic hypogonadism in a homozygous MC4R mutation carrier and the effect of sibutramine treatment on body weight and obesity-related health risks** *Obes Facts* **4**:324–328 https://doi.org/10.1159/000330763

8. Doulla M., McIntyre A.D., Hegele R.A., Gallego P.H (2014) **A novel MC4R mutation associated with childhood-onset obesity: A case report** *Paediatr Child Health* **19**:515–518 https://doi.org/10.1093/pch/19.10.515

9. Batarfi A.A., Filimban N., Bajouh O.S., Dallol A., Chaudhary A.G., Bakhashab S (2019) **MC4R variants rs12970134 and rs17782313 are associated with obese polycystic ovary syndrome patients in the Western region of Saudi Arabia** *BMC Med Genet* **20** https://doi.org/10.1186/s12881-019-0876-x

10. Chen X., Huang L., Tan H.Y., Li H., Wan Y., Cowley M., Veldhuis J.D., Chen C (2017) **Deficient melanocortin-4 receptor causes abnormal reproductive neuroendocrine profile in female mice. Reproduction (Cambridge** *England* **153**:267–276 https://doi.org/10.1530/REP-16-0341

11. Sandrock M., Schulz A., Merkwitz C., Schoneberg T., Spanel-Borowski K., Ricken A (2009) **Reduction in corpora lutea number in obese melanocortin-4-receptor-deficient mice** *Reprod Biol Endocrinol* **7** https://doi.org/10.1186/1477-7827-7-24

12. Cui L. *et al.* (2022) **Dapagliflozin partially restores reproductive function in MC4R KO obese female mice** *The Journal of endocrinology* **254**:65–76 https://doi.org/10.1530/JOE-21-0449

13. Manfredi-Lozano M. *et al.* (2016) **Defining a novel leptin-melanocortin-kisspeptin pathway involved in the metabolic control of puberty** *Mol Metab* **5**:844–857 https://doi.org/10.1016/j.molmet.2016.08.003

14. Goodman R.L., Herbison A.E., Lehman M.N., Navarro V.M (2022) **Neuroendocrine control of gonadotropin-releasing hormone: Pulsatile and surge modes of secretion** *Journal of neuroendocrinology* **34** https://doi.org/10.1111/jne.13094

15. Israel D.D., Sheffer-Babila S., de Luca C., Jo Y.H., Liu S.M., Xia Q., Spergel D.J., Dun S.L., Dun N.J., Chua S.C. (2012) **Effects of leptin and melanocortin signaling interactions on pubertal development and reproduction** *Endocrinology* **153**:2408–2419 https://doi.org/10.1210/en.2011-1822

16. Manfredi-Lozano M., Roa J., Tena-Sempere M (2018) **Connecting metabolism and gonadal function: Novel central neuropeptide pathways involved in the metabolic control of puberty and fertility** *Front Neuroendocrinol* **48**:37–49 https://doi.org/10.1016/j.yfrne.2017.07.008

17. Cravo R.M. *et al.* (2011) **Characterization of Kiss1 neurons using transgenic mouse models** *Neuroscience* **173**:37–56 https://doi.org/10.1016/j.neuroscience.2010.11.022

18. Lam B.Y.H. *et al.* (2021) **MC3R links nutritional state to childhood growth and the timing of puberty** *Nature* **599**:436–441 https://doi.org/10.1038/s41586-021-04088-9

19. Villa P.A., Ruggiero-Ruff R.E., Jamieson B.B., Campbell R.E., Coss D (2024) **Obesity alters POMC and kisspeptin neuron crosstalk leading to reduced luteinizing hormone in male mice** *The Journal of Neuroscience* https://doi.org/10.1523/jneurosci.0222-24.2024

20. Stephens S.B.Z., Kauffman A.S (2021) **Estrogen Regulation of the Molecular Phenotype and Active Translatome of AVPV Kisspeptin Neurons** *Endocrinology* **162** https://doi.org/10.1210/endocr/bqab080

21. Moore A.M., Prescott M., Campbell R.E (2013) **Estradiol negative and positive feedback in a prenatal androgen-induced mouse model of polycystic ovarian syndrome** *Endocrinology* **154**:796–806 https://doi.org/10.1210/en.2012-1954

22. McCarthy E.A. *et al.* (2022) **Inhibiting Kiss1 Neurons With Kappa Opioid Receptor Agonists to Treat Polycystic Ovary Syndrome and Vasomotor Symptoms** *J Clin Endocrinol Metab* **107**:e328–e347 https://doi.org/10.1210/clinem/dgab602

23. Dewailly D., Barbotin A.L., Dumont A., Catteau-Jonard S., Robin G (2020) **Role of Anti-Müllerian Hormone in the Pathogenesis of Polycystic Ovary Syndrome** *Frontiers in endocrinology* **11** https://doi.org/10.3389/fendo.2020.00641

24. Roa J., Herbison A.E (2012) **Direct regulation of GnRH neuron excitability by arcuate nucleus POMC and NPY neuron neuropeptides in female mice** *Endocrinology* **153**:5587–5599 https://doi.org/10.1210/en.2012-1470

25. Zhang C., Bosch M.A., Qiu J., Ronnekleiv O.K., Kelly M.J (2015) **17beta-Estradiol increases persistent Na(+) current and excitability of AVPV/PeN Kiss1 neurons in female mice** *Mol Endocrinol* **29**:518–527 https://doi.org/10.1210/me.2014-1392

26. Clements J.D., Westbrook G.L (1991) **Activation kinetics reveal the number of glutamate and glycine binding sites on the N-methyl-D-aspartate receptor** *Neuron* **7**:605–613 https://doi.org/10.1016/0896-6273(91)90373-8

27. Stincic T.L., Grachev P., Bosch M.A., Rønnekleiv O.K., Kelly M.J (2018) **Estradiol drives the anorexigenic activity of proopiomelanocortin neurons in female mice** *eNeuro* **5**:e0103–118 https://doi.org/10.1523/eneuro.0103-18.2018

28. Qiu J., Nestor C.C., Zhang C., Padilla S.L., Palmiter R.D., Kelly M.J., Rønnekleiv O.K (2016) **High-frequency stimulation-induced peptide release synchronizes arcuate kisspeptin neurons and excited GnRH neurons** *eLife* **5** https://doi.org/10.7554/eLife.16246

29. Qiu J., Rivera H.M., Bosch M.A., Padilla S.L., Stincic T.L., Palmiter R.D., Kelly M.J., Rønnekleiv O.K (2018) **Estrogenic-dependent glutamatergic neurotransmission from kisspeptin neurons governs feeding circuits in females** *eLife* **7** https://doi.org/10.7554/eLife.35656

30. Stincic T.L., Qiu J., Connors A.M., Kelly M.J., Rønnekleiv O.K (2021) **Arcuate and Preoptic Kisspeptin neurons exhibit differential projections to hypothalamic nuclei and exert opposite postsynaptic effects on hypothalamic paraventricular and dorsomedial nuclei in the female mouse** *eneuro, ENEURO.0093-0021.2021* https://doi.org/10.1523/eneuro.0093-21.2021

31. Herman M.A., Ackermann F., Trimbuch T., Rosenmund C (2014) **Vesicular glutamate transporter expression level affects synaptic vesicle release probability at hippocampal synapses in culture** *The Journal of Neuroscience* **34**:11781–11791 https://doi.org/10.1523/JNEUROSCI.1444-14.2014

32. Thornton J.E., Loose M.D., Kelly M.J., Rønnekleiv O.K (1994) **Effects of estrogen on the number of neurons expressing β-endorphin in the medial basal hypothalamus of the female guinea pig** *The Journal of comparative neurology* **341**:68–77 https://doi.org/10.1002/cne.903410107

33. Zhang C., Tonsfeldt K.J., Qiu J., Bosch M.A., Kobayashi K., Steiner R.A., Kelly M.J., Ronnekleiv O.K (2013) **Molecular mechanisms that drive estradiol-dependent burst firing of Kiss1 neurons in the rostral periventricular preoptic area** *American journal of physiology. Endocrinology and metabolism* **305**:E1384–1397 https://doi.org/10.1152/ajpendo.00406.2013

34. Mountjoy K.G., Mortrud M.T., Low M.J., Simerly R.B., Cone R.D (1994) **Localization of the melanocortin-4 receptor (MC4-R) in neuroendocrine and autonomic control circuits in the brain** *Molecular Endocrinology* **8**:1298–1308 https://doi.org/10.1210/mend.8.10.7854347

35. Yu J. *et al.* (2020) **Determination of the melanocortin-4 receptor structure identifies Ca2+ as a cofactor for ligand binding** *Science* **368**:428–433 https://doi.org/10.1126/science.aaz8995

36. Sohn J.W., Harris L.E., Berglund E.D., Liu T., Vong L., Lowell B.B., Balthasar N., Williams K.W., Elmquist J.K (2013) **Melanocortin 4 receptors reciprocally regulate sympathetic and parasympathetic preganglionic neurons** *Cell* **152**:612–619 https://doi.org/10.1016/j.cell.2012.12.022

37. Kelly M.J., Loose M.D., Ronnekleiv O.K (1992) **Estrogen suppresses mu-opioid-and GABAB-mediated hyperpolarization of hypothalamic arcuate neurons** *The Journal of neuroscience : the official journal of the Society for Neuroscience* **12**:2745–2750 https://doi.org/10.1523/JNEUROSCI.12-07-02745.1992

38. Lagrange A.H., Ronnekleiv O.K., Kelly M.J (1994) **The potency of mu-opioid hyperpolarization of hypothalamic arcuate neurons is rapidly attenuated by 17 beta-estradiol** *The Journal of neuroscience : the official journal of the Society for Neuroscience* **14**:6196–6204 https://doi.org/10.1523/JNEUROSCI.14-10-06196.1994

39. Qiu J., Bosch M.A., Tobias S.C., Grandy D.K., Scanlan T.S., Ronnekleiv O.K., Kelly M.J (2003) **Rapid signaling of estrogen in hypothalamic neurons involves a novel G-protein-coupled estrogen receptor that activates protein kinase C** *The Journal of neuroscience : the official journal of the Society for Neuroscience* **23**:9529–9540 https://doi.org/10.1523/JNEUROSCI.23-29-09529.2003

40. Qiu J. *et al.* (2006) **A G-protein-coupled estrogen receptor is involved in hypothalamic control of energy homeostasis** *The Journal of neuroscience : the official journal of the Society for Neuroscience* **26**:5649–5655 https://doi.org/10.1523/jneurosci.0327-06.2006

41. Qiu J., Rivera H.M., Bosch M.A., Padilla S.L., Stincic T.L., Palmiter R.D., Kelly M.J., Ronnekleiv O.K (2018) **Estrogenic-dependent glutamatergic neurotransmission from kisspeptin neurons governs feeding circuits in females** *Elife* **7** https://doi.org/10.7554/eLife.35656

42. Stincic T.L., Grachev P., Bosch M.A., Ronnekleiv O.K., Kelly M.J (2018) **Estradiol Drives the Anorexigenic Activity of Proopiomelanocortin Neurons in Female Mice** *eNeuro* **5** https://doi.org/10.1523/ENEURO.0103-18.2018

43. Ghamari-Langroudi M. *et al.* (2015) **G-protein-independent coupling of MC4R to Kir7.1 in hypothalamic neurons** *Nature* **520**:94–98 https://doi.org/10.1038/nature14051

44. Krause W.C. *et al.* (2021) **Oestrogen engages brain MC4R signalling to drive physical activity in female mice** *Nature* **599**:131–135 https://doi.org/10.1038/s41586-021-04010-3

45. Brix N., Ernst A., Lauridsen L.L.B., Parner E., Stovring H., Olsen J., Henriksen T.B., Ramlau-Hansen C.H (2019) **Timing of puberty in boys and girls: A population-based study** *Paediatr Perinat Epidemiol* **33**:70–78 https://doi.org/10.1111/ppe.12507

46. Padilla S.L., Johnson C.W., Barker F.D., Patterson M.A., Palmiter R.D (2018) **A Neural Circuit Underlying the Generation of Hot Flushes** *Cell Rep* **24**:271–277 https://doi.org/10.1016/j.celrep.2018.06.037

47. Dror T., Franks J., Kauffman A.S (2013) **Analysis of multiple positive feedback paradigms demonstrates a complete absence of LH surges and GnRH activation in mice lacking kisspeptin signaling** *Biology of reproduction* **88** https://doi.org/10.1095/biolreprod.113.108555

48. Steyn F.J., Wan Y., Clarkson J., Veldhuis J.D., Herbison A.E., Chen C (2013) **Development of a methodology for and assessment of pulsatile luteinizing hormone secretion in juvenile and adult male mice** *Endocrinology* **154**:4939–4945 https://doi.org/10.1210/en.2013-1502

49. Talbi R., Ferrari K., Choi J.H., Gerutshang A., McCarthy E.A., Dischino D., Leon S., Navarro V.M (2021) **Characterization of the Action of Tachykinin Signaling on Pulsatile LH Secretion in Male Mice** *Endocrinology* **162** https://doi.org/10.1210/endocr/bqab074

50. Dave J.R., Rubinstein N., Eskay R.L (1985) **Evidence that b-endorphin binds to specific receptors in rat peripheral tissues and stimulates the adenylate cyclase-adenosine 3',5'-monophosphate system** *Endocrinology* **117**:1389–1396

51. Naulé L., Robert V., Parmentier C., Martini M., Keller M., Cohen-Solal M., Hardin-Pouzet H., Grange-Messent V., Franceschini I., Mhaouty-Kodja S (2015) **Delayed pubertal onset and prepubertal Kiss1 expression in female mice lacking central oestrogen receptor beta** *Hum Mol Genet* **24**:7326–7338 https://doi.org/10.1093/hmg/ddv430

52. Pfaffl M.W (2001) **A new mathematical model for relative quantification in real-time RT-PCR** *Nucleic Acids Res* **29** https://doi.org/10.1093/nar/29.9.e45

53. Balthasar N. *et al.* (2004) **Leptin receptor signaling in POMC neurons is required for normal body weight homeostasis** *Neuron* **42**:983–991 https://doi.org/10.1016/j.neuron.2004.06.004

54. Madisen L. *et al.* (2012) **A toolbox of Cre-dependent optogenetic transgenic mice for light-induced activation and silencing** *Nature Neuroscience* **15**:793–802 https://doi.org/10.1038/nn.3078

55. Bosch M.A., Tonsfeldt K.J., Ronnekleiv O.K (2013) **mRNA expression of ion channels in GnRH neurons: subtype-specific regulation by 17beta-estradiol** *Molecular and cellular endocrinology* **367**:85–97 https://doi.org/10.1016/j.mce.2012.12.021

56. Qiu J., Nestor C.C., Zhang C., Padilla S.L., Palmiter R.D., Kelly M.J., Ronnekleiv O.K (2016) **High-frequency stimulation-induced peptide release synchronizes arcuate kisspeptin neurons and excites GnRH neurons** *Elife* **5** https://doi.org/10.7554/eLife.16246

57. Stincic T.L., Qiu J., Connors A.M., Kelly M.J., Ronnekleiv O.K (2021) **Arcuate and Preoptic Kisspeptin Neurons Exhibit Differential Projections to Hypothalamic Nuclei and Exert Opposite Postsynaptic Effects on Hypothalamic Paraventricular and Dorsomedial Nuclei in the Female Mouse** *eNeuro* **8** https://doi.org/10.1523/ENEURO.0093-21.2021

58. Qiu J., Stincic T.L., Bosch M.A., Connors A.M., Kaech Petrie S., Ronnekleiv O.K., Kelly M.J (2021) **Deletion of Stim1 in Hypothalamic Arcuate Nucleus Kiss1 Neurons Potentiates Synchronous GCaMP Activity and Protects against Diet-Induced Obesity** *The Journal of neuroscience : the official journal of the Society for Neuroscience* **41**:9688–9701 https://doi.org/10.1523/JNEUROSCI.0622-21.2021

Editors

Reviewer #1 (Public Review):

Summary:

The authors investigate the role of the melanocortin system in puberty onset. They conclude that proopiomelanocortin (POMC) neurons within the arcuate nucleus of the hypothalamus provide important but differing input to kisspeptin neurons in the arcuate or rostral hypothalamus.

Strengths:

- innovative and novel
- technically sound
- well-designed
- thorough

Weaknesses:

There were no major weaknesses identified.

https://doi.org/10.7554/eLife.100722.1.sa3

Reviewer #2 (Public Review):

Summary:

This interesting manuscript describes a study investigating the role of MC4R (melanocortin 4 receptor) signalling on kisspeptin (Kiss1) neurons. The initial question is a good one. Infertility in human MC4R mutations has typically been ascribed to the consequent obesity and impaired metabolic regulation. Whether MC4R directly regulates the hypothalamic-pituitary-gonadal (HPG) axis has not been thoroughly examined. Here, the researchers assembled an elegant combination of loss and gain of function in vivo experiments, specifically targeting MC4R expression in Kiss1 neurons. This is an excellent experimental design and one that should provide compelling evidence for whether there is a direct role for melanocortin signalling in arcuate Kiss1 neurons to support normal reproductive function. There were definite effects on reproductive function (irregular estrous cycle, reduced magnitude of LH surge induced by exogenous estradiol). Still, the magnitude of these responses and the overall effect on fertility were relatively minor, as mice lacking MC4R in Kiss1 neurons remained fertile despite these irregularities. The second part of the manuscript describes a series of electrophysiological studies evaluating the pharmacological effects of melanocortin signalling in Kiss1 neurons in ex-vivo brain slides. These studies characterised interesting differential actions of melanocortins in two different Kiss1 neuronal populations. The study provides some novel insights into how direct actions of melanocortin signalling via the MC4R in Kiss1 neurons contribute to the metabolic regulation of the reproductive system. Importantly, however, it is clear that other mechanisms are also at play.

Strengths:

The loss and gain of function experiments provide a conceptually simple but hugely informative experimental design, which is the key strength of the current paper - especially the knock-in study that showed improved reproductive function even in the presence of ongoing obesity. This is a very convincing result that documents that reproductive deficits in MC4R knockout animals (and humans with deleterious MC4R gene variants) can be ascribed to impaired signalling in the hypothalamic Kiss1 neurons and not necessarily simply caused

as a consequence of obesity. Validation experiments for these studies are needed, given their great prominence in the manuscript, because these are critical to interpretation.

Weaknesses:

(1) Given the fact that mice lacking MC4R in Kiss1 neurons remained fertile despite some reproductive irregularities, the overall tone and some of the conclusions of the manuscript (e.g., from the abstract: "... Mc4r expressed in Kiss1 neurons is required for fertility in females") were overstated. Perhaps this can be described as a contributing pathway, but other mechanisms must also be involved in conveying metabolic information to the reproductive system.

(2) The mechanistic studies evaluating melanocortin signalling in Kiss1 neurons were all completed in ovariectomised animals (with and without exogenous hormones) that do not experience cyclical hormone changes. Such cyclical changes are fundamental to how these neurons function in vivo and may dynamically alter the way they respond to neuropeptides. Therefore, eliminating this variable makes interpretation difficult.

(3) Use of the POMC-Cre to target ontogenetic inputs to Kiss1 neurons might have targeted a wider population of cells than intended.

https://doi.org/10.7554/eLife.100722.1.sa2

Reviewer #3 (Public Review):

The manuscript by Talbi R et al. generated transgenic mice to assess the reproduction function of MC4R in Kiss1 neurons in vivo and used electrophysiology to test how MC4R activation regulated Kiss1 neuronal firing in ARH and AVPV/PeN. This timely study is highly significant in the field of neuroendocrinology research for the following reasons.

(1) The authors' findings are significant in the field of reproductive research. Despite the known presence of MC4R signaling in Kiss1 neurons, the exact mechanisms of how MC4R signaling regulates different Kiss1 neuronal populations in the context of sex hormone fluctuations are not completely understood. The authors reported that knocking out Mc4r from Kiss1 neurons replicates the reproductive impairment of MC4RKO mice, and Mc4r expression in Kiss1 neurons in the MC4R null background partially restored the reproductive impairment. MC4R activation excites Kiss1 ARH neurons and inhibits Kiss1 AVPV/PeN neurons (except for elevated estradiol).

(2) Reproduction dysfunction is one of obesity comorbidities. MC4R loss-of-function mutations cause obesity phenotype and impaired reproduction. However, it's hard to determine the causality. The authors carefully measured the body weight of the different mouse models (Figure 1C, Figure 2A, Figure 3B). For example, the Kiss1-MC4RKO females showed no body weight difference at the age of puberty onset. This clearly demonstrated the direct function of MC4R signaling in reproduction but was not a consequence of excessive adiposity.

(3) Gene expression findings in the "KNDy" system are in line with the reproduction phenotype.

(4) The electrophysiology results reported in this manuscript are innovative and provide more details of MC4R activation and Kiss1 neuronal activation.

Overall, the authors have presented sufficient background in a clear and logically organized structure, clearly stated the key question to be addressed, used the appropriate methodology, produced significant and innovative main findings, and made a justified conclusion.

https://doi.org/10.7554/eLife.100722.1.sa1

Author response:

We are grateful to the reviewers and the editorial team for their feedback and thorough revisions of our paper. We also appreciate their acknowledgement that this study represents a significant advancement in the field of reproductive neuroendocrinology and offers insights on the contribution of obesity vs melanocortin signaling in women's fertility. In the revised version, we will provide a more detailed clarification of the data and methodology and adhere to the reviewers' suggestions.

Please find below our answers to specific concerns in the public review:

> *Given the fact that mice lacking MC4R in Kiss1 neurons remained fertile despite some reproductive irregularities, the overall tone and some of the conclusions of the manuscript (e.g., from the abstract: "... Mc4r expressed in Kiss1 neurons is required for fertility in females") were overstated. Perhaps this can be described as a contributing pathway, but other mechanisms must also be involved in conveying metabolic information to the reproductive system.*

We will tone down these statements throughout the manuscript to indicate that MC4R in Kiss1 neurons plays a role in the metabolic control of fertility (rather than "…is required for fertility")

> *The mechanistic studies evaluating melanocortin signalling in Kiss1 neurons were all completed in ovariectomised animals (with and without exogenous hormones) that do not experience cyclical hormone changes. Such cyclical changes are fundamental to how these neurons function in vivo and may dynamically alter the way they respond to neuropeptides. Therefore, eliminating this variable makes interpretation difficult.*

Mice lack true follicular and luteal phases and therefore it is impossible to separate estrogen-mediated changes from progesterone-mediated changes (e.g., in a proestrous female). Therefore, we use an ovariectomized female model in which we can generate a LH surge with an E2-replacement regimen [1]. This model enables us to focus on estrogen effects, exclude progesterone effects, and minimize variability. Inclusion of cycling females would make interpretation much more difficult.

(1) Bosch et al., 2013 Mol & Cell Endo; https://doi.org/10.1016/j.mce.2012.12.021

> *Use of the POMC-Cre to target ontogenetic inputs to Kiss1 neurons might have targeted a wider population of cells than intended.*

POMC is transiently expressed during embryonic development in a portion of cells fated to be Kiss1 or NPY/AgRP neurons [1-2]. Therefore, this is a valid concern when crossing with a floxed mouse. However, use of AAVs in adult animals avoids this issue and leads to specific expression in POMC neurons [3]. This POMC-Cre mouse has been used extensively with AAVs to drive specific expression in POMC neurons by other laboratories [4-7]. Therefore, we are confident that our optogenetic studies have narrowly targeted POMC inputs.

(1) Padilla et al., 2010 Nat Med; https://doi.org/10.1038/nm.2126

(2) Lam et al., 2017 Mol Metab; https://doi.org/10.1016/j.molmet.2017.02.007

(3) Stincic et al., 2018 eNeuro; https://doi.org/10.1523/eneuro.0103-18.2018

(4) Fenselau et al., 2017 Nat Neuro; https://doi.org/10.1038/nn.4442

(5) Rau & Hentges, 2019 J Neuro; https://doi.org/10.1523/jneurosci.3193-18.2019

(6) Fortin et al., 2021 Nutrients; https://doi.org/10.3390/nu13051642

(7) Villa et al., 2024 J Neuro; https://doi.org/10.1523/jneurosci.0222-24.2024

https://doi.org/10.7554/eLife.100722.1.sa0